MICROCOPY RESOLUTION TEST CHART
NATIONAL BUREAU OF STANDARDS-1963-A

LEVEL II ⑫ 12
SC

AD A093151

LOW—LOSS INFRARED FIBERS

James A. Harrington

Hughes Research Laboratories
3011 Malibu Canyon Road
Malibu, CA 90265

December 1980

DTIC
DEC 17 1980
E

Approved for public release; distribution unlimited

80 12 15 172

REPORT DOCUMENTATION PAGE	READ INSTRUCTIONS BEFORE COMPLETING FORM

1. REPORT NUMBER	2. GOVT ACCESSION NO.	3. RECIPIENT'S CATALOG NUMBER
	AD-A093 757	

4. TITLE (and Subtitle)	5. TYPE OF REPORT & PERIOD COVERED
LOW-LOSS INFRARED FIBERS.	Final Report. 1 Aug 79 - 26 Sept 80
	6. PERFORMING ORG. REPORT NUMBER

7. AUTHOR(s)	8. CONTRACT OR GRANT NUMBER(s)
A. Harrington	N00173-79-C-0348

9. PERFORMING ORGANIZATION NAME AND ADDRESS	10. PROGRAM ELEMENT, PROJECT, TASK AREA & WORK UNIT NUMBERS
Hughes Research Laboratories 3011 Malibu Canyon Road Malibu, CA 93065	59

11. CONTROLLING OFFICE NAME AND ADDRESS	12. REPORT DATE
Defense Advanced Research Projects Agency Arlington, VA 22209	December 1980
	13. NUMBER OF PAGES
	63

14. MONITORING AGENCY NAME & ADDRESS(if different from Controlling Office)	15. SECURITY CLASS. (of this report)
Naval Research Laboratory Washington, DC 20375	UNCLASSIFIED
	15a. DECLASSIFICATION DOWNGRADING SCHEDULE

16. DISTRIBUTION STATEMENT (of this Report)

Approved for public release; distribution unlimited.

17. DISTRIBUTION STATEMENT (of the abstract entered in Block 20, if different from Report)

18. SUPPLEMENTARY NOTES

19. KEY WORDS (Continue on reverse side if necessary and identify by block number)

Fiber optics, Infrared fibers, Optical transmission lines, Infrared materials.

20. ABSTRACT (Continue on reverse side if necessary and identify by block number)

This final report describes research on low-loss fiber waveguides for use in future long-distance fiber links. The goal of the program is to develop non-oxide-containing fibers with losses as low as 10^{-3} dB/km. This work is part of an overall technology assessment to determine the feasibility of fabricating such ultra-low-loss optical fibers. —next page

DD FORM 1473 EDITION OF 1 NOV 65 IS OBSOLETE

Cont.

The approach being used to develop these very transparent waveguides is to fabricate fiber from IR transmitting crystalline materials. The materials studied were the alkali and thallium halides. We found that we could not successfully apply our extrusion technology, developed for the thallium halides, to fabricate alkali halide fibers. Extruded KCl or CsI fibers, for example, always had poor surface quality due to surface cracks (fish-scale appearance). We therefore abandoned extrusion methods for the alkali halides in favor of other fiber fabrication techniques.

An alternative technique used was single crystal (SC) fiber growth. SC fibers represent a potentially ideal waveguide because they are free from mechanical defects (such as strain fields associated with grain boundaries in extruded polycrystalline fibers) and thus should have less scattering losses than polycrystalline waveguides. To make SC fibers we used an inverted Czochralski growth technique and applied the method to KCl. By the end of the program we had not yet produced any SC KCl fiber, but we expect to do so shortly.

The optical losses in our extruded KRS-5 (TlBrI) fiber were evaluated and related to the mechanical and structural properties of the fiber. We found that the recrystallization temperature of the fiber (3 μm average grain size) is 105°C and that fiber transmission decreases as the fiber is bent in a loop. This decrease is caused by parting at grain boundaries. We also calculated the zero materials dispersion for our crystalline materials.
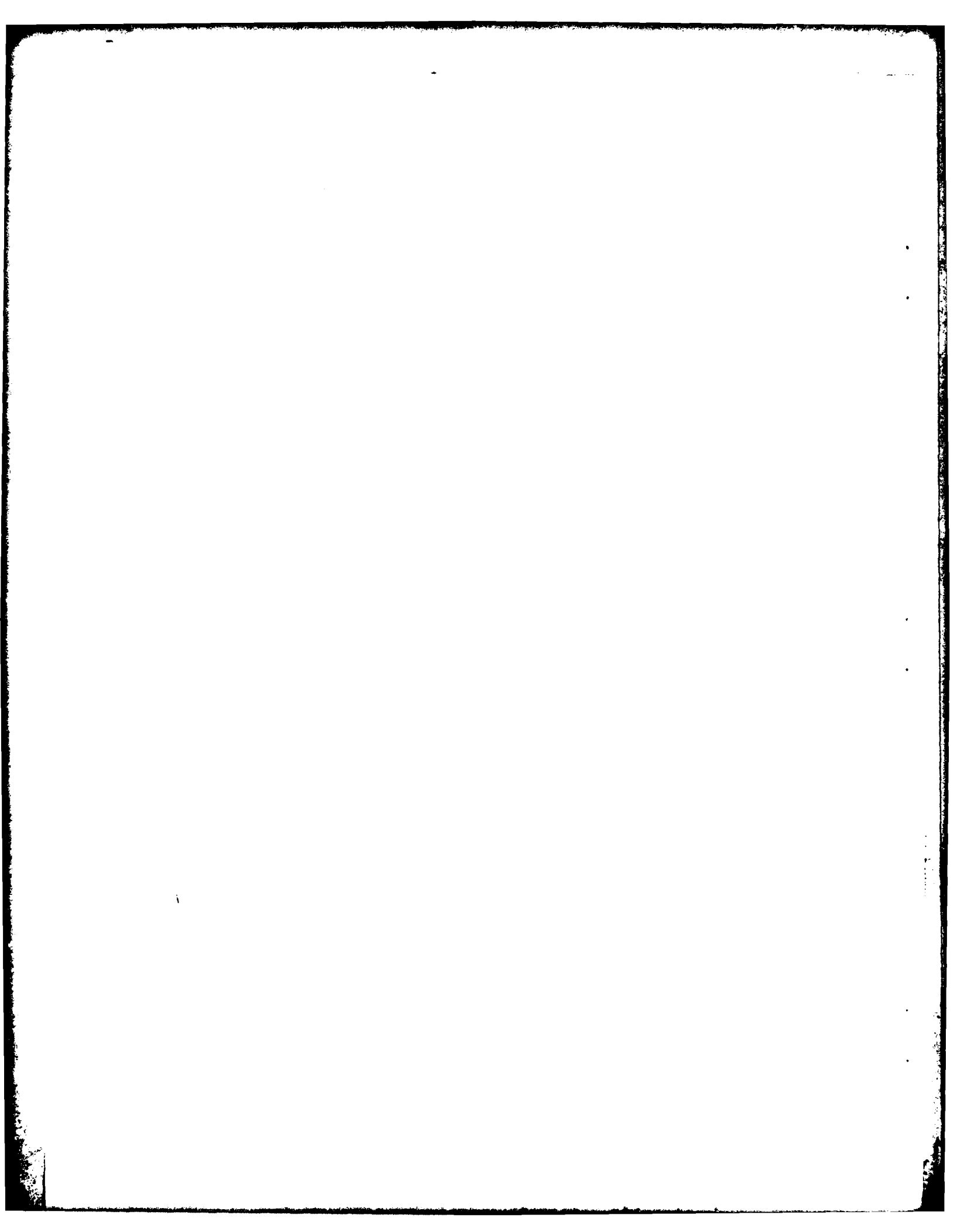
PREFACE

This final technical report describes work on low-loss IR fiber waveguides performed during the period 1 August 1979 to 26 September 1980. This period covers our part of the first phase of a technology assessment designed to evaluate the feasibility of fabricating ultra-low-loss IR fibers for future needs.

The principal investigator was James A. Harrington. Overall program coordination was provided by D. Michael Henderson.

Participating in the research program were the following personnel: Arlie Standlee extruded the KCl and KRS-5 fiber and performed the optical measurements; Roger Turk and Nelson Ramirez made the mechanical measurements; Tony Pastor and Tino Lee performed the single crystal fiber studies; and Jim Harrington and Mike Henderson carried out the analysis.

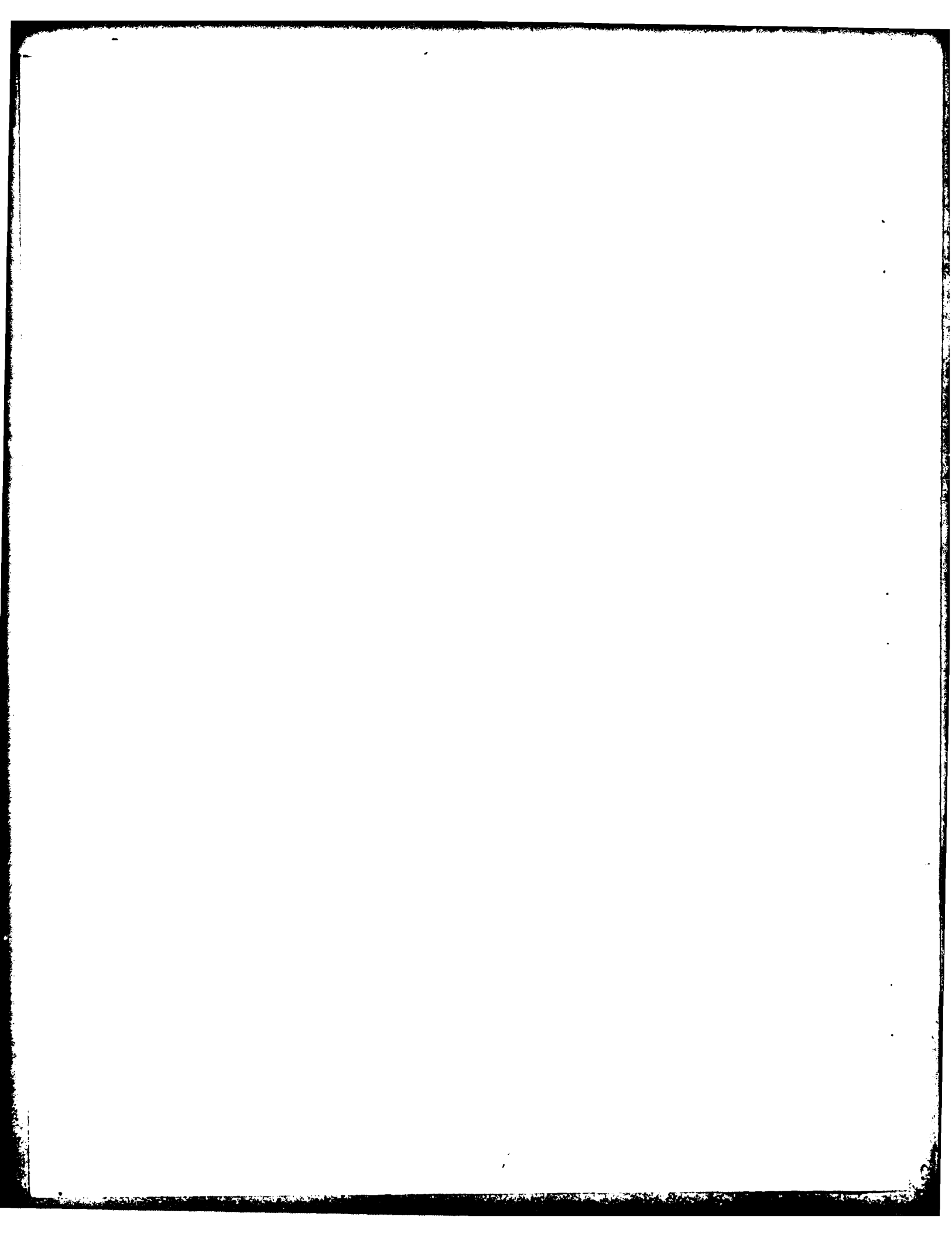| Accession For	
NTIS GRA&I	☒
DDC TAB	☐
Unannounced	☐
Justification_____	
By_____	
Distribution/	
Availability Codes	
Dist	Avail and/or special
A	

3

LIST OF ILLUSTRATIONS

LIST OF ILLUSTRATIONS

SECTION 1

INTRODUCTION AND SUMMARY

Current long distance communications links employing silica fibers are limited, by material losses, to lengths no greater than 100 km. Communication systems now envisioned, however, will require repeaterless links thousands of kilometers long. To meet these future needs will require developing fiber waveguides from non-oxide (silica type) materials whose potential loss is as low as 10^{-3} dB/km. The primary objective of this research program is to develop a new class of fibers from highly transparent crystalline materials. This is part of an overall technology-assessment effort to determine the feasibility of fabricating ultra-low-loss optical fibers with losses near 10^{-3} dB/km.

The approach we have taken to develop these very transparent waveguides is to fabricate fiber from our best IR transmitting crystalline materials. Initially, we chose to study KCl because this material had exhibited the lowest loss measured to date for a non-oxide crystal[1] (absorption coefficient equal to 10^{-6} cm^{-1} or 4.0 dB/km at 5.3 μm). To form a fiber from this material, we used our existing extrusion press because extrusion had proven so successful for the thallium halides.[2-4] After an extensive 2-year research program (funded in large part by RADC), our results for extruded KCl were not encouraging. The KCl fiber was found to have poor surface quality (fish-scale appearance), and the best transmission we obtained was 4,200 dB/km (on a 20-cm length of 500-μm-diameter fiber) — far above the program goal. Therefore, we decided to abandon the extrusion of KCl in favor of other fiber fabrication techniques.

Two techniques other than extrusion appear promising for preparing alkali or other metal halide fibers. One of these is hot rolling to form polycrystalline fibers; the other is single-crystal (SC) fiber growth. In this program we initiated a study on the growth of SC KCl fibers. Our approach to SC fiber growth was unique because the fibers were grown in a reactive atmosphere process (RAP)[5] environment used to maintain the purity of the KCl. After studying three different methods

9

of growing SC fibers in a RAP environment, we selected one, an inverted Czochralski procedure, for implementation. We made several attempts at growth but were unable before the end of the program to produce any SC KCl fiber. But we believe that the design of the apparatus has been improved sufficiently so that a short (30 cm) length of SC KCl will soon be obtained. We feel strongly that SC fibers are potentially very low in loss because the scattering and absorptive losses in such an ideal waveguide would be very small.

An important part of our investigation of low-loss IR fiber has been an evaluation of the optical and mechanical properties of selected crystalline materials. Our calculations[3,4] show that KCl and KRS-5 (TlBrI), as well as many other halide materials,[6] have projected theoretical losses near 5 μm that are several orders of magnitude below that of silica.[4] The best IR fibers, however, have losses that are 3 to 5 orders of magnitude greater than the theoretical predictions for these materials[3,4] (KRS-5 fiber loss is 400 dB/km at 10 μm). To reach the program goal of 10^{-3} dB/km, extrinsic losses — those resulting from chemical impurities, mechanical imperfections, and irregularities in the fiber's surface — must be greatly reduced. This program has examined one particular aspect of extrinsic loss mechanisms: the relationship between certain mechanical and structural properties of polycrystalline KRS-5 fiber and the fiber's transmission. Our measurements involving fiber grain size and temperature revealed that the recrystallization temperature of KRS-5 fiber is 105°C and that substantial grain growth will occur in fibers left for hours at this temperature (grain size increased by a factor of 8). In another set of experiments, we found that the transmission degraded when the fiber was subjected to a loop stress (10% decrease for a 20-cm-diameter loop in 250-μm-diameter KRS-5 fiber). This information led us to conclude that polycrystalline fibers are inherently limited by problems associated with grain boundaries. The fibers part at grain boundaries, which we suspect causes the decrease in transmission observed in our flexure experiments. In addition, the instability of fiber grain size with time and temperature implies that the fiber will weaken over time, which would be deleterious

in future applications. For these reasons, we will pursue SC fiber technology to meet our goals.

Specifically, we recommend the following directions for the next phase of this program to assess ultra-low-loss technology:

- Stop all work to fabricate polycrystalline fibers by extrusion. We feel that the polycrystalline guides will be too lossy because of problems associated with grain boundaries (mechanical weakness, excess scattering from strain fields, etc.).

- Develop SC fiber technology for the Tl halides. The Tl halides are particularly attractive because they are ductile, readily form fiber, and do not cleave (alkali halides do).

- Continue to evaluate and analyze bulk and fiber materials. This should include careful analysis of absorptive and scattering losses and the correlation of these losses with both starting material purity and fabrication technique.

- Develop RAP chemistry methods for purifying the Tl halides. These techniques have proven so successful for the alkali halides that we must now apply similar methods to KRS-5, TlBr, etc. to obtain better fiber material.

11
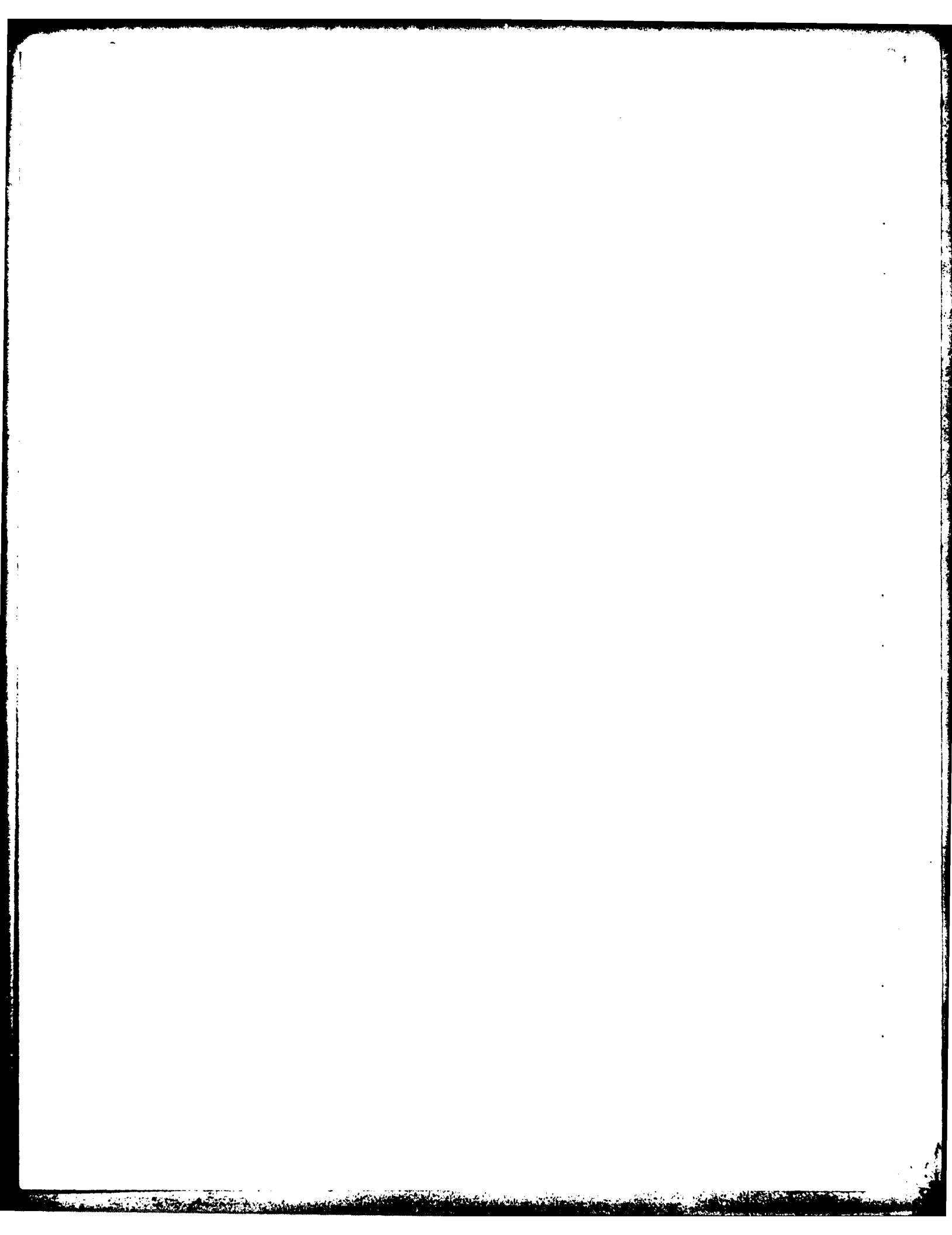
SECTION 2

TECHNICAL PROGRESS AND DISCUSSION

A. GENERAL CONSIDERATIONS

The development of next-generation, ultra-low-loss fibers for
long-distance communication links requires using a new class of non-
oxide-containing materials and unconventional fiber fabrication methods.
Present silica or other oxide glass fibers have, in many cases, losses
equal to the projected theoretical losses for these materials. In partic-
ular, silica fiber has a measured loss of 0.25 dB/km at 1.6 μm.[7] Fig-
ure 1 shows the projected transmission of silica plotted along with that
of KCl and KRS-5 (TlBrI), two candidate materials for ultra-low-loss
fibers. These data show that the measured loss in silica occurs at the
minimum in the V-shaped loss curve; this indicates that no further
improvement in silica fiber transmission is possible. Figure 1 also
shows, however, that certain crystalline materials (KCl and KRS-5 are
only two of these) have theoretical losses well below that of silica.
In this research program, we are exploiting the theoretical advantage of
these and other halide crystalline materials to fabricate — by extrusion,
hot rolling, and single-crystal growth — fibers from materials with pro-
jected losses in the 10^{-3} dB/km range.

Although the V curve for silica plotted in Figure 1 has been verified
experimentally, the predicted losses for the halide materials are still
far below present IR fiber losses. The best IR fiber to date has been
KRS-5, which has a measured loss of 400 dB/km at 10.6 μm.[4] This is
approximately three orders of magnitude above the intrinsic loss at
10 μm (see V curve in Figure 1) and well above the minima at 5 μm. We
feel that these excess losses result from impurities in the material and
nonoptimized fabrication methods. In this program, we attempted to use
the highest purity materials available and devised new methods, such as
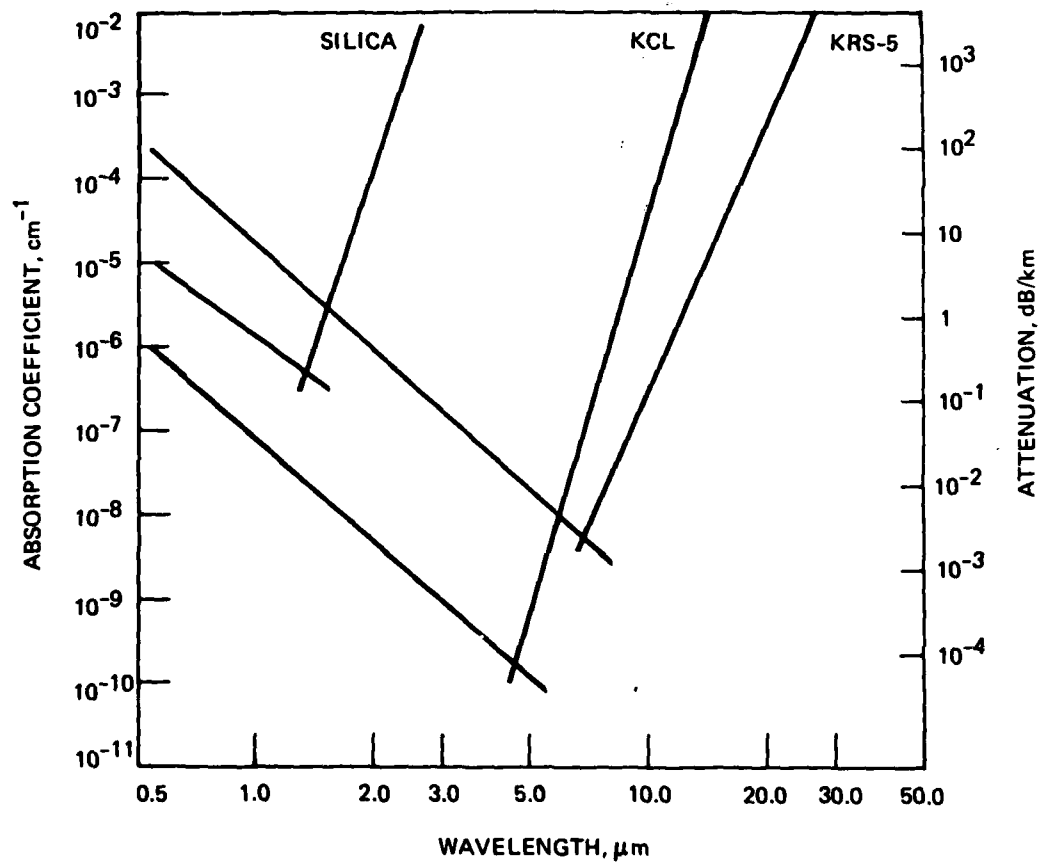SC fiber growth, in an attempt to overcome the current IR fiber
limitations.

Figure 1. Projected transmission in IR fibers.

In developing highly transparent waveguides, the researcher is confronted with a large class of potentially low-loss materials. On the surface, it would appear that the 20 alkali halides (group IA-VII) would be excellent candidates, in part because of their already established low absorption in some bulk crystals.[1] Of the 20 alkali halides, we would in fact select KCl as an ideal candidate based on transparency alone, for KCl has exhibited the lowest loss[1] (10^{-6} cm^{-1} = 0.4 dB/km at 5.3 μm) of any material at IR wavelengths. As discussed in Section 2.B, however, KCl proved intractable for <u>extrusion</u> into good-quality fiber. All 20 alkali halides and certain of their physical properties are listed in Table 1. In addition to KCl, the more ductile CsI (lower melting point, MP) is also a good candidate.

Materials other than the alkali halides that are suitable for IR fibers are special (non-oxide) glasses such as $ZnCl_2$,[6] BeF_2,[6] and halide glasses[8,9] and the more ductile crystalline materials such as the Tl[4] and Ag[10] halides. The multicomponent fluoride glasses (an example of which is ZrF_4-ThF_4-B_aF_2)[8] have the obviously attractive capability of being drawn into fiber. One group has drawn 34 m of fluoride glass fiber, and their lowest loss for a 1 m sample of fiber was 0.45 dB/m at 3.39 μm.[11] Although fluoride glasses are potentially very exciting because they are amenable to conventional glass fiber forming technologies, there do remain numerous problems to be solved before low-loss fibers are produced. Experimentally, the temperature range in which these materials form glass is narrow, which results in frequent devitrification of both fiber and bulk material. On the theoretical side, virtually nothing is known about scattering losses in these materials. We expect, however, that Rayleigh scattering is a significant loss mechanism due to both inherent scattering from density fluctuations present in all glasses and scattering from compositional fluctuations resulting from the multicomponent nature of the glasses. (Some fluoride glasses have as many as seven components!)

The Tl and Ag halides are particularly attractive candidates not only because their projected losses (see Figure 1) are low, but also because they are more ductile than the alkali halides. We have our most

Table 1. Physical Properties of 20 Alkali Halides

VII \ IA		Li	Na	K	Rb	Cs
F	M_p =	870°C	992°C	880°C	760°C	683°C
	ρ =	2.60g/cm^3	2.79	2.50	2.88	3.58
	n =	1.35 (3.8 μm)	1.23 (10.6 μm)	1.36 (0.57 μm)	1.35 (10 μm)	1.44 (10 μm)
	Hardness =	102 Knoop	60			
	Solubility =	0.27g/100g H$_2$O	4.2g/100g H$_2$O	92.3g/100g H$_2$O	130.6g/100g H$_2$O	367g/100g H$_2$O
Cl	M_p =	614°C	800°C	790°C	715°C	460°C (tr); 646 (β)
	ρ =	2.06g/cm^3	2.16	1.99	2.76	3.988
	n =	1.53 (10 μm)	1.48 (10 μm)	1.45 (10.6 μm)	1.47 (10 μm)	1.61 (10 μm)
	Hardness =		18	8		
	Solubility =	63.7g/100g H$_2$O	36g/100g H$_2$O	34.3g/100g H$_2$O (0°)	77g/100g H$_2$O (0°)	186g/100g H$_2$O
Br	M_p =	547°C	755°C	730°C	682°C	636°C
	ρ =	3.46g/cm^3	3.21	2.75	3.35	4.43
	n =	1.69	1.58 (10 μm)	1.52 (10.6 μm)	1.52 (10 μm)	1.66
	Hardness =			7		19.5
	Solubility -	63.7g/100g H$_2$O	91g/100g H$_2$O	65.2g/100g H$_2$O	98g/100g H$_2$O (5°)	124g/100g H$_2$O
I	M_p =	466°C	651°C	723°C	642°C	621°C
	ρ =	4.06g/cm^3	3.66	3.11	3.55	4.51
	n =	1.92	1.72 (10 μm)	1.62	1.61 (10 μm)	1.74 (10 μm)
	Hardness =					5
	Solubility =	165g/100g H$_2$O	179g/100g H$_2$O	144g/100g H$_2$O	152g/100g H$_2$O	44g/100g H$_2$O (0°C)

extensive IR fiber technology base in the Tl halides (in particular KRS-5), and we feel that extruded KRS-5 is a very good fiber for near-term (short length) applications. As we show in Section 2.B, however, extrusion is a very rough process mechanically and hence is probably unsuitable for non-ductile materials. For this reason, we have decided to explore SC fibers as a means of producing the ultimate transparent waveguide for long-distance applications.

B. FIBER EXTRUSION TECHNOLOGY

1. KCl Fibers — A Review

Our initial approach to fabricating low-loss fiber involved extruding KCl fiber. As explained above, the primary motivation for choosing KCl was the availability of ultrapure single-crystal KCl (purified using RAP) with the lowest losses measured to date at IR wavelengths. Beginning with RAP KCl, we extruded numerous KCl fibers under a variety of experimental conditions. To summarize, we extruded (1) unlubricated KCl from 25 to 740°C, (2) lubricated KCl (best lubricant Parafilm M, which is a mixture of polyetheylene and parafin), and (3) KCl into an inert atmosphere (Cerechor). The KCl fiber produced from this effort (funded in large part by RADC under contract F19628-78-C-0109) always had poor surface quality. The KCl surfaces were fish scaled, which led, as expected, to poor transmission (high scattering losses). Figure 2 shows the irregular surface structure present in unlubricated KCl — a structure that persists even at high extrusion temperatures (740°C) very near the MP for KCl (790°C). We found that lubricated KCl fiber had less of a fish-scale appearance because the lubricants reduced the friction between the extrusion die and KCl (friction leads to surface tearing and microcleavage cracks in the fiber); but, once the lubricant was removed, the surface of the fiber was still poor. Our lowest loss KCl fiber (coated with Parafilm M lubricant) had a loss of 4.20 dB/m at 10.6 μm. From this study we concluded that extrusion is not a viable fiber fabrication method for KCl. Furthermore, we believe, based on the extrusion of other alkali halides, that it is probably not applicable to alkali halides in general.

17

● 500 μm DIAMETER
● 100X MAGNIFICATION

300°C   400°C   740°C
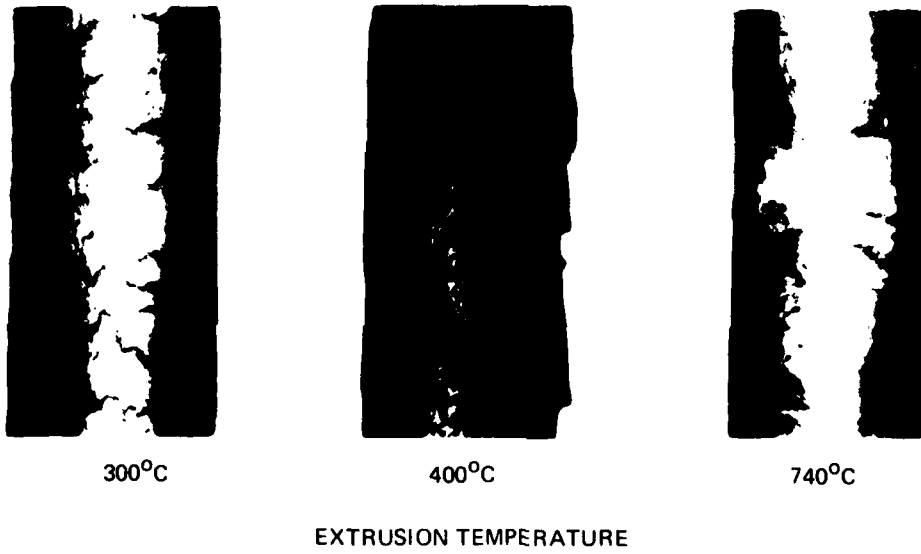
EXTRUSION TEMPERATURE

Figure 2.   High-temperature extrusion of KCl fiber.

18

2. CsI Fibers

To determine if there are alkali halides that in fact are amenable
to extrusion into fiber, we decided to extrude CsI. We note from Table 1
that CsI has a significantly lower MP than KCl (621°C versus 790°C) and
is more ductile. It would, therefore, seem reasonable to suspect that
CsI would produce less friction as it passes through the die and thus the
surface of the film would experience less tearing. Beginning with an
unlubricated billet (5.3 mm diameter, 7.0 cm long) of Harshaw single-
crystal CsI, we extruded 500-μm-diameter fiber at temperatures between
200 and 500°C. All of the fiber had the rough, irregular surface charac-
teristic of extruded KCl fiber. The surface was so rough that the fiber
appeared white. Etching the CsI fiber to reveal the microstructure
showed the surface to be somewhat pitted (see Figure 3). We believe that
this is due to attack by moisture; this problem is more serious in CsI
fiber than in KCl fiber because CsI is more soluble (see Table 1). The
grain size of the polycrystalline fibers is quite evident in Figure 3.
Table 2 shows the curious result for these fibers that the average grain
size does not increase as the extrusion temperature is increased. If,
however, the 200°C grain size is anomalous (i.e., too large), then the
grain size increases with temperature, as expected. This is the usual
result observed for Tl halide and KCl fibers. In general, CsI has not
yielded fiber with smooth surfaces. This result coupled with our data
on KCl fibers reinforces our position that the alkali halides are not
extrudable.

Table 2. Grain Sizes for Extruded
CsI Fiber

Extrusion Temperature, °C	Grain Size, μm
200	140
260	84
350	98
500	100

19
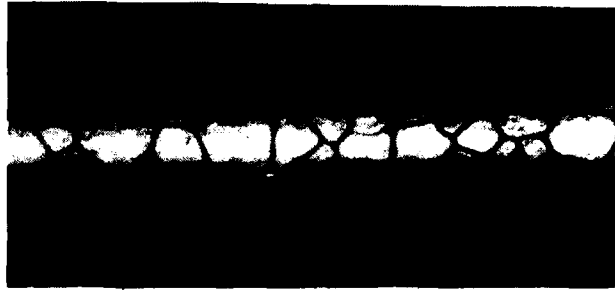
Figure 3(a).
CsI fiber (500 μm diameter) extruded at
260°C.

Figure 3(b).
CsI fiber (500 μm diameter) extruded at
350°C. Note pitting produced by moisture.

Figure 3(c).
CsI fiber (500 μm diameter) extruded at
500°C.

3. ZnSe Fiber

Zinc selenide has been used as a low-loss IR window material for
many years. We felt that this material might be extrudable into fiber
even though it is considerably more brittle than the halide materials.
To extrude ZnSe, however, requires high extrusion temperatures because
the MP of ZnSe is high (1525°C). To achieve a high extrusion temperature,
we used our high temperature heater and carefully insulated the heater
and die assembly.

The starting billet of ZnSe was cut from Raytheon CVD material. A
500-μm-diameter diamond die (~100:1 area reduction) was used and the
extrusion temperature was 800°C (maximum temperature). Applying a maxi-
mum force of 24 kN, we were not able to extrude fiber through the die.
Instead, some of the ZnSe squirted out between the diamond die holder
and the main die assembly. At these pressures and temperatures, we found
that materials would weaken, thus leading to an opening through which
the ZnSe could flow more readily than through the diamond die. At this
time, we feel that it is unwise to go to even higher extrusion tempera-
tures because of weakness in the materials making up the extrusion
assembly. In addition, at these elevated temperatures, materials like
ZnSe, GaAs, and CdTe may decompose with the result that fiber material
would not be stoichiometric. In particular, GaAs should probably not be
extruded above 600°C since As might be given off. Given these considera-
tions, it seems reasonable to abandon actively pursuing the extrusion
of ZnSe, GaAs, CdTe, or other similar semiconducting materials.

4. KRS-5 Fiber

The foundation of our IR fiber technology is the extrusion of KRS-5
fiber. Over the past four years, we have made numerous extrusions of
this material and, as mentioned in Section 2.A, this is our best IR fiber.
The optical and mechanical properties of this fiber have been well
documented (see the Appendix for further background).[4]

In this program, several KRS-5 fiber extrusion runs were made to
provide fiber for our optical and mechanical testing. The unclad KRS-5

fiber extruded was either 250 or 500 μm in diameter in lengths ranging from 1 to 2 m. Figures 4 and 5 show an overview and detail of the controls of our extrusion press. Using this press, we can extrude ~25 m of 250-μm-diameter fiber in one run. Generally, the fiber is removed in 1- to 2-m lengths as it is extruded, although the fiber can be automatically wound on the take-up reel (see Figure 4) if desired. Immediately after extrusion, the fiber is evaluated optically using our 10.6-μm insertion-loss apparatus (shown diagrammed in Figure 6). The fibers used in this study had losses from 0.8 to 2.0 dB/m.

5. Optical and Mechanical Properties of KRS-5 Fiber

The important mechanical properties of fibers studied include tensile strength and grain size. Although some work has been done on these basic properties (see the Appendix), we have extended these results to include other fiber diameters and a wider range of grain sizes. To prepare fiber with different grain sizes for mechanical testing, we used two techniques. The first method (discussed in the Appendix) involves extruding the fiber at different extrusion temperatures (200 to 350°C) and at different quench gas temperatures (LN_2 cooled N_2 to room temperature). The second uses a post-extrusion anneal (described below). With these methods, we have prepared fiber with average grain sizes between 3 and 50 μm.

The KRS-5 fiber was tensile tested using our Instron machine. A typical stress-strain curve for KRS-5 fiber, which has an average grain size of 3 μm, is shown in Figure 7. These data show the large region of plastic flow (anelasticity) typical of our polycrystalline fibers. The photomicrographs at the top of Figure 7 indicate the failure mechanisms of the fiber. At some point in the elongation (presumably near the fracture or ultimate failure point), the fiber grains begin to part (Figure 7(b)). When the fiber fractures, the individual grains are clearly revealed (Figures 7(c) and 7(d)). Interestingly, the optical transmission does not degrade dramatically as one moves from the linear (Hooke's law) to the anelastic region of a fiber. Instead, we find that the transmission decreases monotonically as stress increases (see discussion below).

22
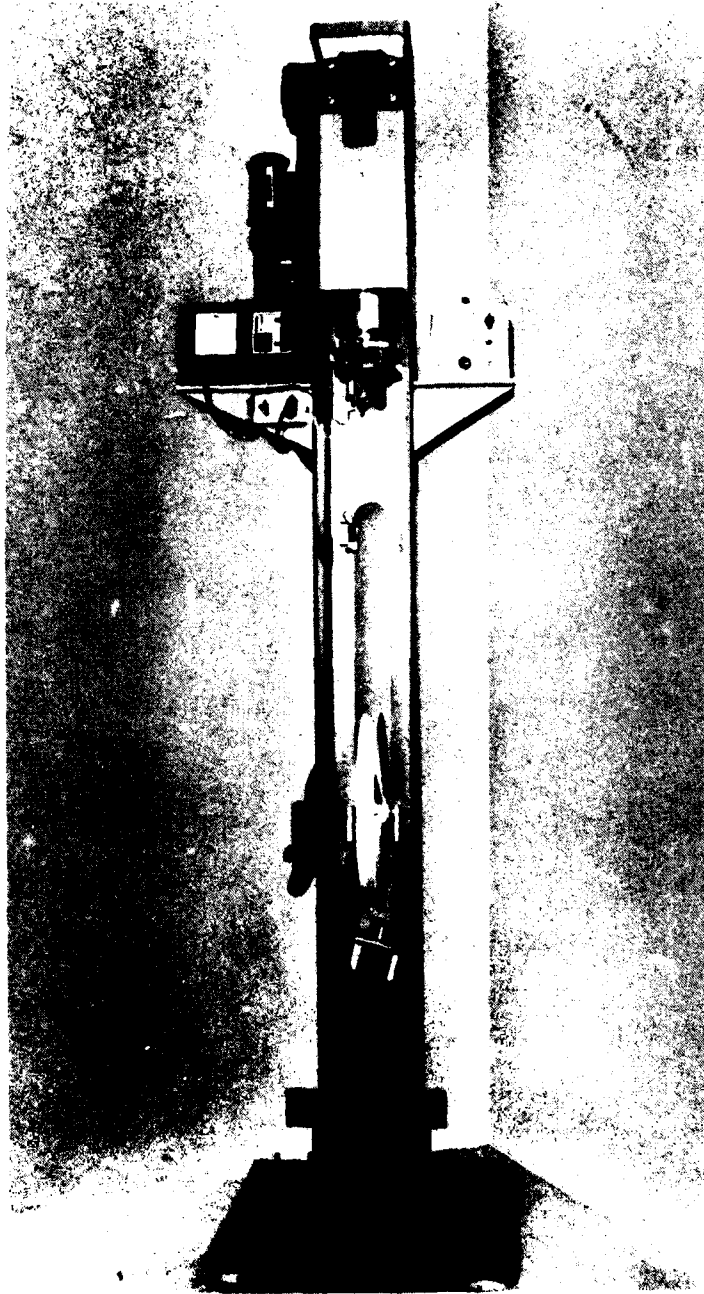
Figure 4. Overall view of extruder showing controls and fiber take-up reel.
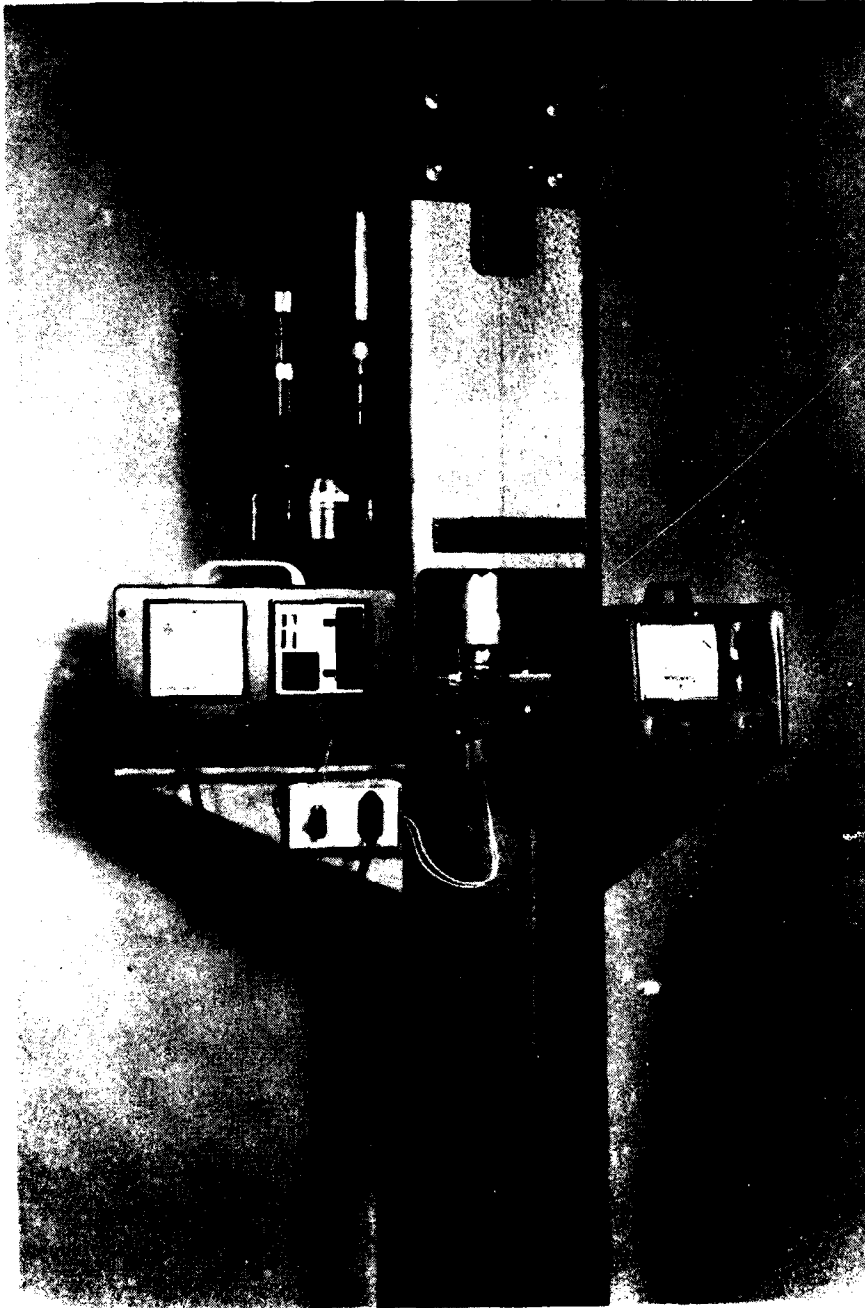
Figure 5. Detail of extruder controls showing temperature
and pressure controls and extrusion chamber.

POWER METER
I_o

POWER METER
I

fl 2.5 cm
ZnSe LENS

XYZ MICRO-
POSITIONER

STABILIZED
CO_2 LASER

IR FIBER

f4
OPTICS

ZnSe
BEAM SPLITTER

SHUTTER

POLARIZER

HALF-WAVE
PLATE

POWER
SUPPLY
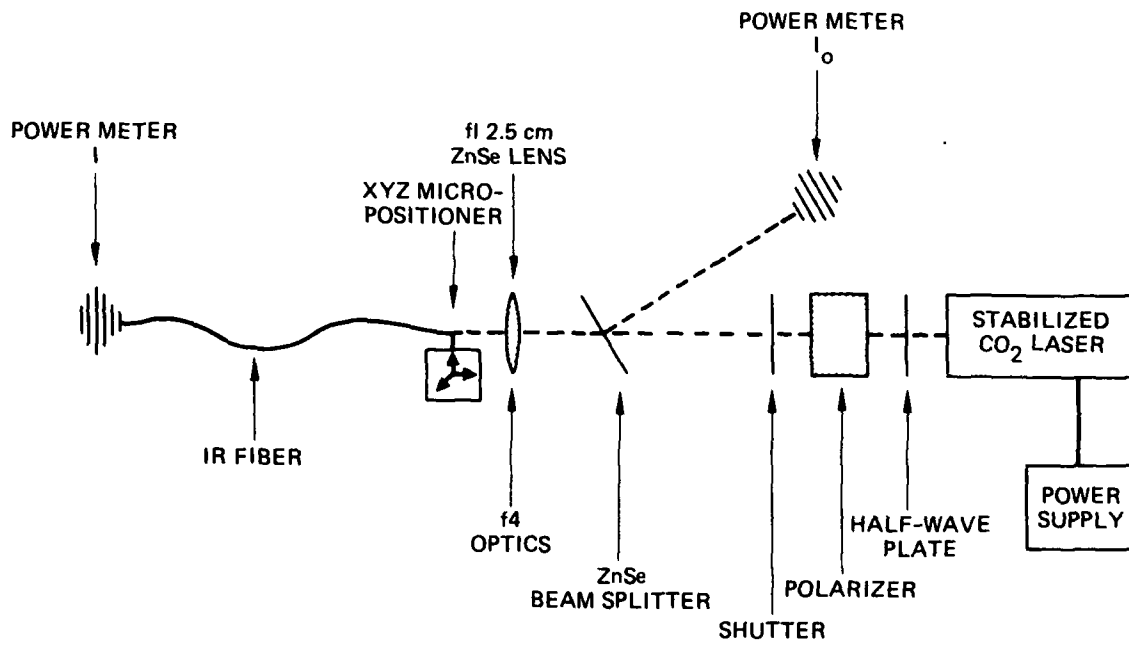
Figure 6.   IR fiber loss measurement apparatus.

Figure 7. Tensile test data for KRS-5 fiber.

A. ORIGINAL STRUCTURE, 500X
NOTE EQUIAXED GRAINS

B. MODE OF "PLASTIC FLOW," 500X
NOTE GRAIN BOUNDARY SEPARATION

C. SURFACE

D. END

9508-2

FRACTURE OCCURS ALONG
GRAIN BOUNDARIES, 500X

TYPICAL LOAD VS ELONGATION CURVE,
250 μm DIAMETER FIBER

CROSSHEAD SPEED = 0.01 cm/min
GAGE LENGTH = 8 cm

ELONGATION , mm

APPLIED LOAD , g

300

200

100

0

0.5   1.0   1.5   2.0   2.5   3.0

26

Data such as those given in Figure 7 for a fiber grain size of 3 μm were taken for other grain sizes. These data, presented in Figure 8 for a 250-μm-diameter fiber and in the Appendix for a 100-μm-diameter fiber, lead to several important conclusions. First and most important, fiber strength increases as the grain size decreases. This is as predicted by the empirical Hall-Petch relation ($\sigma_y \propto d^{-1/2}$, where σ_y is the average grain size), although in Figure 8 this dependence is not obeyed at the smallest fiber grain sizes. Below 7 μm grain size, fiber strength levels off rather than increases. An explanation for this effect lies in the ultimate failure mechanism for these fibers: parting at grain boundaries (see Figure 7(d)). Because the grain boundaries are weaker than the material (usually not the case in polycrystalline metals), there will be a point where the added strength resulting from smaller grains will be exactly compensated for by the weakness caused by increasing the density of grain boundaries through smaller grain sizes. Figure 8 suggests that this point seems to be at a grain size of about 6 to 7 μm. Below this size, any further decrease in the grain size will not strengthen the fiber further. We conclude that greater fiber strength will result from using smaller grain size fibers unless the grain boundaries themselves are strengthened (such as by adding an impurity ion).

We also note from Figure 8 that the curves for yield and ultimate strength diverge at smaller grain sizes. This follows from the mode of plastic flow of KRS-5: separation at grain boundaries. At the yield point, finer grains yield locally by boundary separation, but, since crack propagation is impeded by the fine-grained structure, a higher ultimate strength is reached after considerable elongation in the form of grain-boundary opening. Large grains separate at the yield point to form openings that rapidly connect to cause failure with very little elongation. These curves will intersect when grain size approaches fiber diameter.

Figure 8 and Figure 5 in the Appendix show that the larger (250-μm-diameter) fiber had a greater yield strength than the smaller (100-μm-diameter) fiber. This most likely results because separation starts at
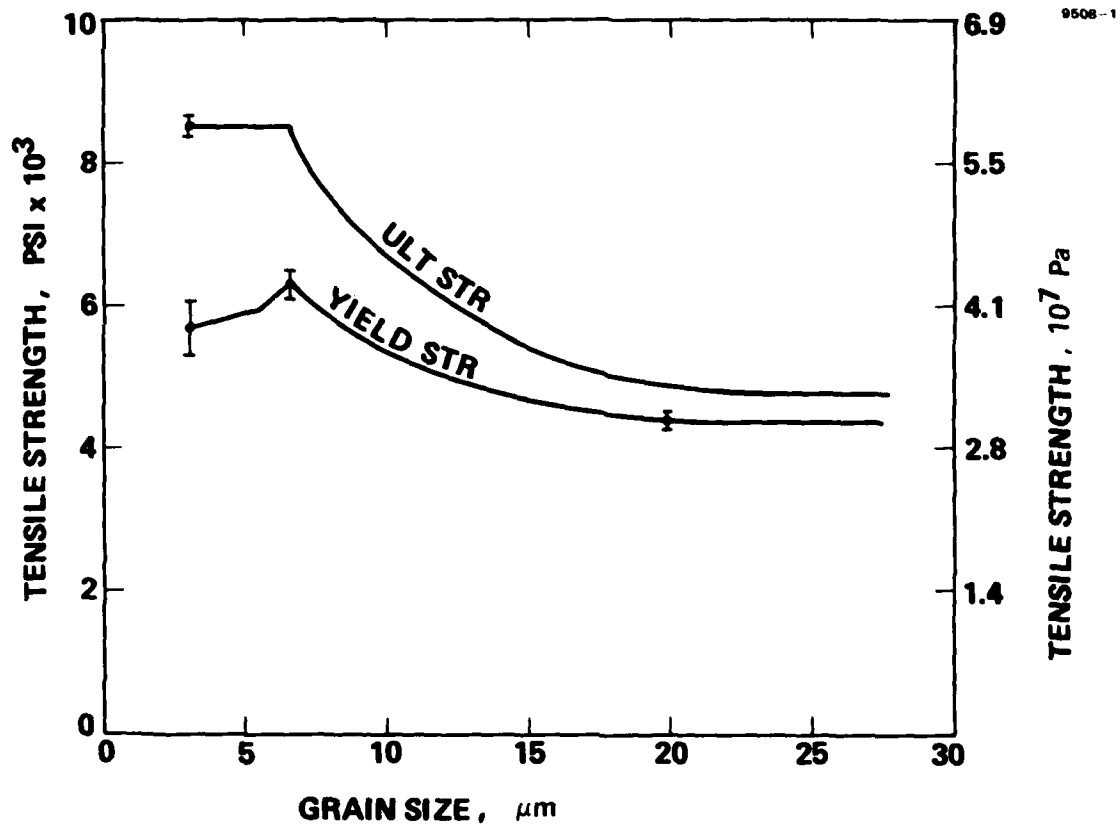
27

Figure 8. Mechanical strength of 250-μm-diameter KRS-5 fiber.

surface boundaries, and the smaller fiber, which has a higher percentage of boundaries intersecting the surface, yields at a lower unit stress.

Our studies of structural properties were concerned with establishing the grain growth pattern with respect to thermal conditioning. In the first experiment, lengths of KRS-5 fiber (250 μm diameter) were heat treated at five temperatures between 100 to 127°C for 15 min. Figure 9 show the resulting grain growth. In this cycle, the average grain size increased from 4.1 μm (room temperature through 100°C) to 10.0 μm at 127°C. We conclude from these limited data that the recrystallization temperature (the temperature where grains begin to grow) for this fiber is about 105°C. This temperature is dependent on the fiber grain size and the extrusion parameters used in fabricating the fiber.

Using this information on recrystallization temperature, we performed another experiment to determine the effect of heating KRS-5 fiber for an extended time. These data along with the recrystallization point data enable us to predict how the strength of our fiber will be affected in applications involving thermal cycling. The data for thermally soaking 250-μm-diameter KRS-5 fiber at a constant temperature of 105°C are given in Figure 10. Again beginning with 4.1 μm grain size fiber, the grain size increased markedly after 1 to 2 hr. After 16 hr, the grain size had increased to 24.9 μm. Figure 10 indicates that the sharpest increase in grain size occurred between 1 and 5 hr. Between 5 hr (17.6 μm) and 16 hr (24.9 μm), the fiber grain size began to level off. Clearly, if given sufficient time, grain size should approach an asymtotote as the thermal energy supplied becomes less than the energy required for grain growth. The data also indicate that the fiber can withstand short (less than 1 hr) periods of 105°C heat without its structural properties being greatly affected.

The mechanical and structural properties (strength and grain size) of a fiber can also be related to its optical properties. This is in general rather complex because of the many interrelationships involved, but we have made an initial attempt to study this by investigating the fiber's transmission while under tensile stress. In doing this, we hoped to learn how loading a fiber affects its loss.
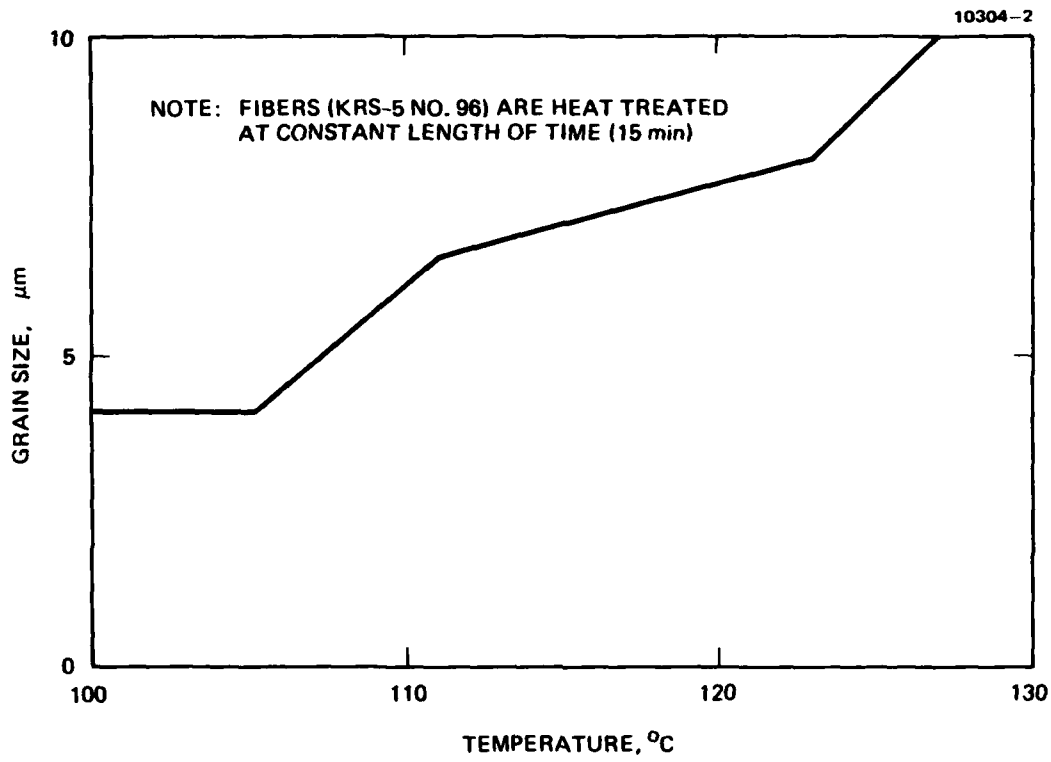
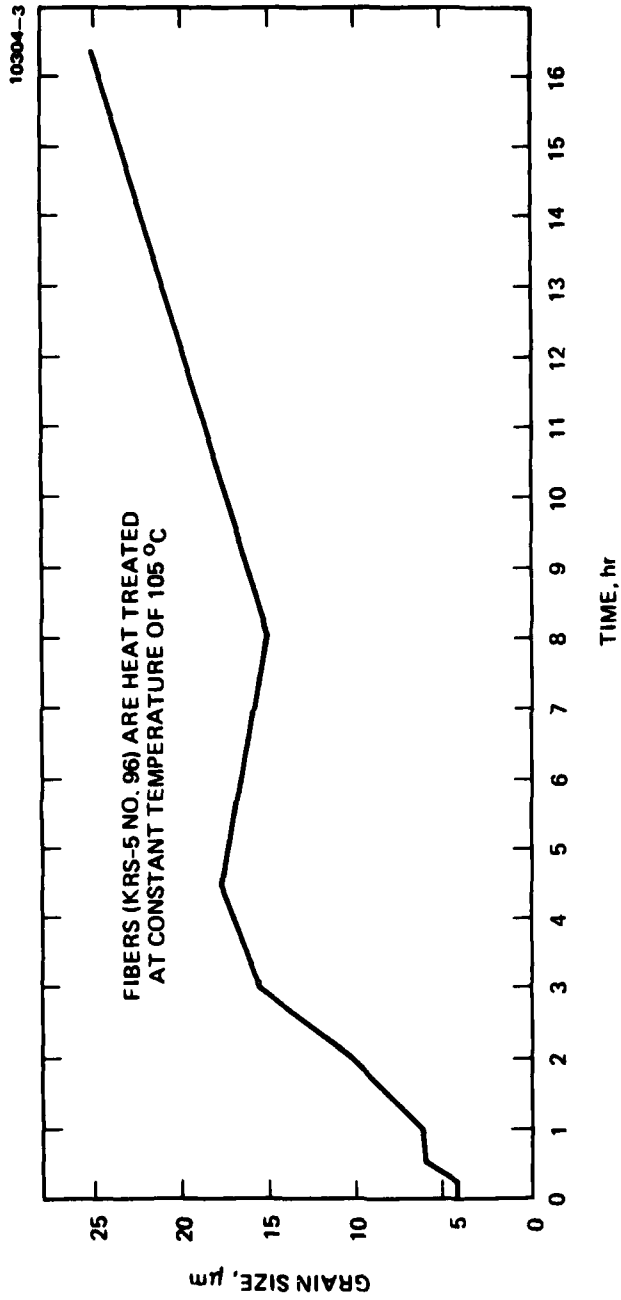Figure 9.   Annealing of KRS-5 fiber for constant time periods.

Figure 10. Annealing KRS-5 fiber at constant temperature.

31

The simplest way to obtain this information is to apply a uniform load to the fiber, as illustrated in the stress-strain data in Figure 7, while measuring the transmission. We would expect a priori that the fiber would exhibit one behavior in the linear (Hooke's law) region and another, appreciable effect as the fiber is plastically deformed (see Figure 7). For ease of experimentation, we decided to put a loop (of diameter D) in the fiber (of diameter d) while the fiber is illuminated by the CO_2 laser (insertion loss measurement). The loop stress σ is then given by:

$$\sigma = \frac{Ed}{D} \tag{1}$$

for

$$\sigma < \sigma_y \quad ,$$

where E is Young's modulus. This formula is only applicable to the proportional limit (yield point). The smallest diameter of the loop, D_y, that can be placed in the fiber with Eq. 1 still valid can be estimated from the data in Figure 7 and the measured value of E (for 250-μm-diameter fiber, 1.16×10^6 psi). Using $\sigma = \sigma_y = 5.9 \times 10^3$ psi and Eq. 1, we find that D_y is equal to 4.7 cm. At smaller loop diameters, the fiber is plastically deformed (when restraightened, the fiber is found to have a permanent bend or set in it).

To relate load data (up to the yield point) to fiber transmission, we measured loss as a function of loop diameter. The data are summarized in Figure 11. The fiber was 250-μm-diameter, 170-cm-long KRS-5; the initial loss was 1.50 dB/m. The figure shows that the loss increased monotonically through the yield point and into the anelastic region. There was no observable discontinuity in the loss at the yield point. Also, when restraightened, the fiber's transmission usually did not return to its original value regardless of whether the loop diameter was greater (linear region) or less (anelastic region) than D_y. We interpret this
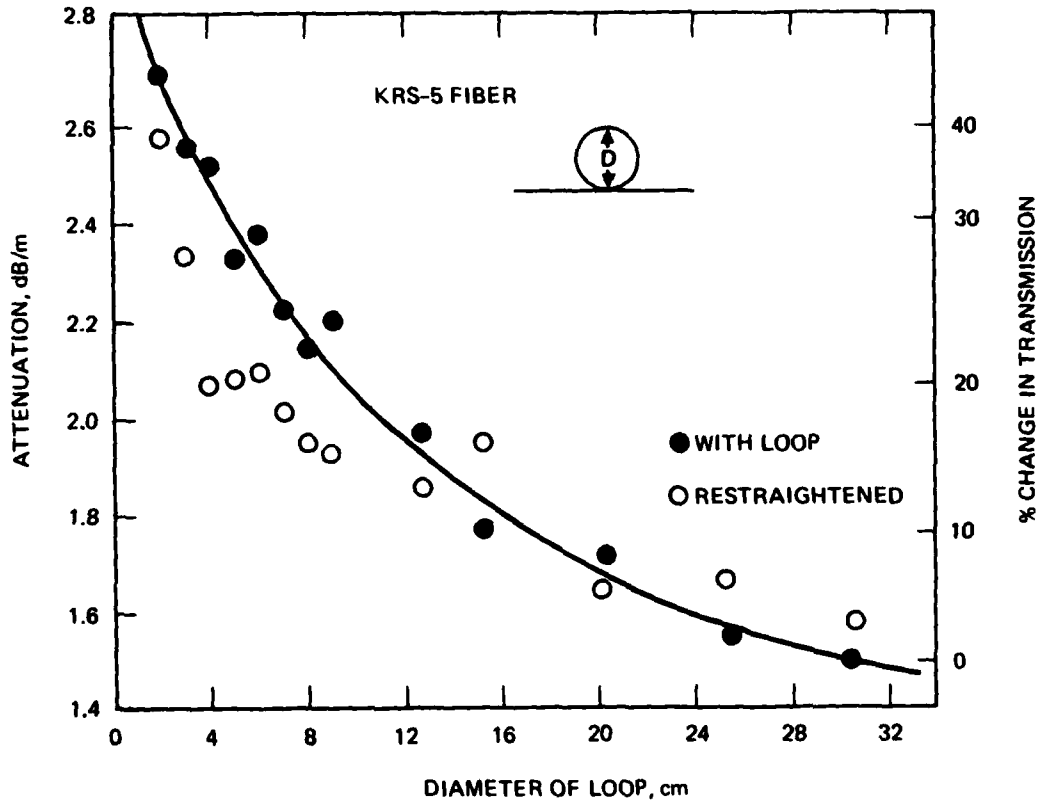
Figure 11. Transmission of KRS-5 fiber under loop stress.

hysteresis as being due to grain boundary separation or changes in residual strain fields under load (leads to scattering). In passing, we note that the fiber transmission remained within 10% of its initial value for loop diameters greater than 18 cm (σ at 18 cm is 1.45×10^3 psi). Finally, this experiment was a very simple attempt to correlate tensile stress and bend radius with fiber loss. Further experiments are needed to determine the relation between grain size, residual strain (strain birefringence), and true tensile stress on optical properties (absorption and scattering losses).

C.   SINGLE-CRYSTAL TECHNOLOGY

1.   Overview

Early during this research program, we demonstrated that it is not feasible to extrude alkali halide fibers. Therefore, we began to develop new fiber-fabrication techniques for forming alkali or other metal halide fibers. The method we selected for extensive study was single-crystal fiber growth. We felt that SC fibers offered the greatest potential for ultra-low loss, primarily because scattering losses should be extremely small for this type of structure. We began by assessing three possible methods for making SC fibers (at first in short, ~12-in.-lengths). After reviewing the chemical kinetics and advantages of each, we chose Czochralski growth of KCl fibers for our first attempt. But we failed to pull any fiber due to the difficulty in seeding the melt. Thus, we devoted the majority of the effort to inverted Czochralski growth. And although we have been unable to grow any SC fiber using this method, we continue to feel that the principle is sound and that SC fibers will be produced in the near future. This section presents our ideas and preliminary experiments designed to produce SC KCl (RAP purified) fiber.

2. Czochralski Growth of KCl Fibers

To achieve SC growth with a uniform cross section to lengths that
are many orders of magnitude greater than the cross-sectional diameter,
the crystal growth system must be capable of maintaining steady-state
operation through the desired length of crystal. During steady-state
Czochralski growth of a crystal, the melt in the vicinity of the growth
interface must be held steadily at its melting point. The growth
interface acts as an isothermal heat source, itself at the melting
point, and steady-state growth will progress only if the latent heat of
crystallization issuing from this source is channeled away from the melt
side of the growth interface at a rate matching the growth rate of the
crystal. This matching of heat production and heat sinking rates is
expressable as a heat balance equation. If it is assumed that the heat
is withdrawn from the interface exclusively by thermal conduction
longitudinally through the growing crystal, the heat balance across the
interface will yield an expression for the growth rate:

$$\dot{R} = \frac{kM}{\rho H_c} \frac{dT}{dz} \quad , \tag{2}$$

where k is the thermal conductivity of the crystal in the growth direc-
tion, M is its molecular weight, ρ is its density at or just below its
melting point, H_c is its molar latent heat of crystallization, and
dT/dz is the longitudinal thermal gradient in the crystal just above the
growth interface.

That this model of steady-state Czochralski growth is oversimplified
becomes apparent when it is noted that there are only two variables in
Eq. 2, $\dot{R}$ and dT/dz, related to each other linearly, so that $\dot{R}$ may be
increased without limit merely by increasing dT/dz. This absurdity
results from the fact that the heat-balance equation involves only the
equilibrium states before and after the phase transformation and does
not allow for the finite rate at which the transformation itself takes
place. This inadequacy of the model can be compensated for by assuming

35

that there exists a maximum value of $\dot{R}$ (characteristic of the growth
material), corresponding to a maximum value of dT/dz (characteristic of
the crystal growth system), beyond which single-crystal growth is not
feasible. Clearly, a crystal growth system would not be adequate for the
growth of monocrystalline filaments unless it could provide this limiting
value of the temperature gradient dT/dz on the crystal of the desired
composition and configuration. Now consider the constraint in the steady-
state model that the efflux of heat is confined solely to the conductive
mode in the direction of the crystal axis (i.e., that there is negligibly
little or no lateral heat loss from the crystal through conduction in
the radial direction and from the exposed surface of the crystal through
radiation and convection). These questions should be considered. Is
this condition really necessary? If so, is it practicable?

Figure 12(a) shows the crystal-melt system at and around the growth
interface for the contrary situation — transverse heat flow. The curved
lines with the arrowheads on them represent some heat flow lines, and
the growth interface is drawn as an isothermal surface that is every-
where orthogonal to the heat flow lines. (Isotropicity of thermal con-
ductivity in the solid is assumed in this descriptive treatment.) The
direction of crystal growth at each point on this surface is normal to it
and is therefore parallel, but countercurrent, to the heat flow line at
that point. It is worth noting that a spurious nucleation at any point
on the growth interface — except on the crystal axis — will result in
spurious growth propagation into the crystal. Bubbles, for example,
would tend to converge at the crystal axis and cause the crystal to
become hollow, or tubular. Furthermore, because of the tendency of the
crystal to grow inward even at the edge of the growth interface, a
delicate balance between the growth rate and the pull rate would have
to be maintained to keep the diameter of the growing crystal constant.
In other words, steady-state growth would be difficult or impossible to
achieve. Therefore, radiative-convective cooling must be reduced to
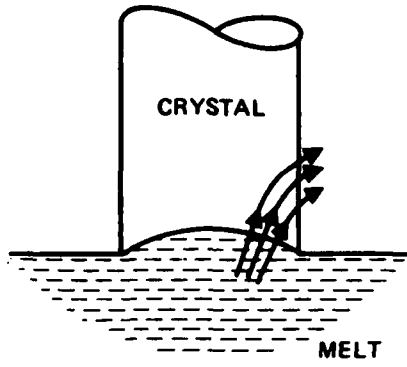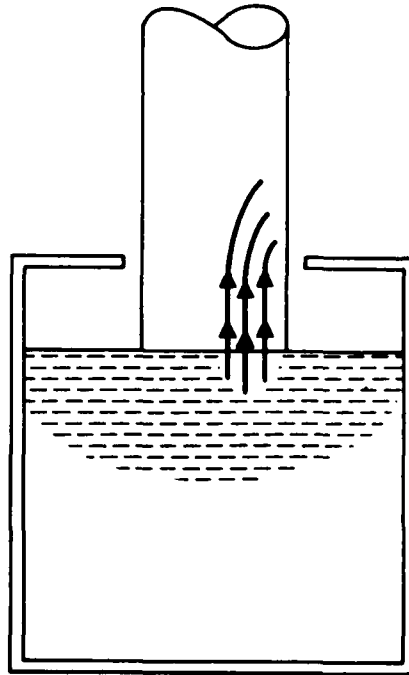negligible proportions if steady-state growth is to be realized.

36

Figure 12(a).
Crystal-melt system at interface.

Figure 12(b).
Schematic of Czochralski growth
system.

A further point about concave-interface operation is noteworthy. Even assuming that steady-state growth were achieved under these conditions (i.e., $\dot{R}$ is the same, in the axial direction, everywhere on the interface and is constant through time), the growth rate along the direction of growth would vary from point to point on the interface. Such growth conditions are conducive to variations in defect concentrations over the cross section of the grown crystal, which may be manifested as optical inhomogeneity of the crystal.

Figure 12(b) shows schematically a system that demonstrates the practicability of the Czochralski operation, in which radiative-convective losses near the growth interface are reduced to negligible levels. The crucible and baffle (drawn as one continuous piece) are made of highly thermally conductive material and therefore its temperature tends to remain uniform. The vapor space inside the crucible functions as an isothermal enclosure and prevents radiative heat loss from that segment of the crystal near the growth interface. The amount of convection loss is limited by the volume of that vapor space and the free area at the opening in the baffle.

The design of our first KCl fiber puller was based on the preceding considerations. Although the proper size of the baffle opening had to be determined by trial-and-error experimentation, there were practical minimum limits to its size imposed by the diameter of the pulling rod and the misalignment between the axes of the pulling rod and the baffle. (Incidentally, it is this unavoidable eccentricity that the rotation of the puller is meant to compensate for, but this feature will have to be avoided in a full-scale system; the present system has been designed to pull to a maximum range of 10 in.)

Our plan for KCl fiber pulling was to establish the minimum diameter of KCl filament that could be pulled through each of the three orifices. Unfortunately, the heating element burned out before we could nucleate our first growth. And, the localized overheating resulting from the burnout also caused damage to the crucible itself.

Another method used to pull SC fibers is related to one used by Bridges et al.[12] for growing SC AgBr fibers. Although that method does conform to the steady-state growth conditions outlined above, it has not been adapted to the RAP environment required for KCl fibers. Rather, Bridges et al. prepared their fibers in air, and their fiber losses were high ($\sim 1 \times 10^{-2}$ cm^{-1}). Since converting a non-RAP system to a RAP system is a major change, we have designed all these systems to use a RAP environment.

Figure 13 shows the RAP-modified Bridges system. The principal feature to note is that the system has two separate vapor chambers; within each chamber a steady-state gas flow will have to be maintained. Although these two chambers are separated, they are not independent. The hydrostatic pressure differential between these two chambers will determine the rate at which the melt flows through the capillary tubing and hence the rate at which the filament grows. Therefore, it is essential to have precise control instrumentation to monitor that pressure differential.

The diagram is only a schematic. The fact that no provision is shown for introducing the charge material into the melting chamber is not meant to imply that this would be only a trivial problem in designing the apparatus. The limitation to the length of fiber specimens that can be pulled, which is implicit in the diagram, is quite real, however. Although a winding spool could conceivably be enclosed in the uppermost chamber to replace the pulling rod, this would entail expanding the volume of that chamber, which would reduce the system's sensitivity to the pressure differential control instrument.

Figure 14 shows the third system schematically. In this system, gavity favors the flow of melt through the capillary tube in the growth direction. We know from experience that RAP potassium chloride melt does not wet fused-silica surfaces that have also been subjected to RAP treatment. Therefore, the melt should not leak spontaneously through the capillary tube if the inside diameter of that tube is sufficiently small; our experience suggests that 0.3 mm is small enough. In this inverted configuration, we expect that the rate of flow of melt through

39

10304-6

SEAL

SEAL

INERT GAS IN →

→ INERT GAS OUT

PULLING
ROD

GROWTH
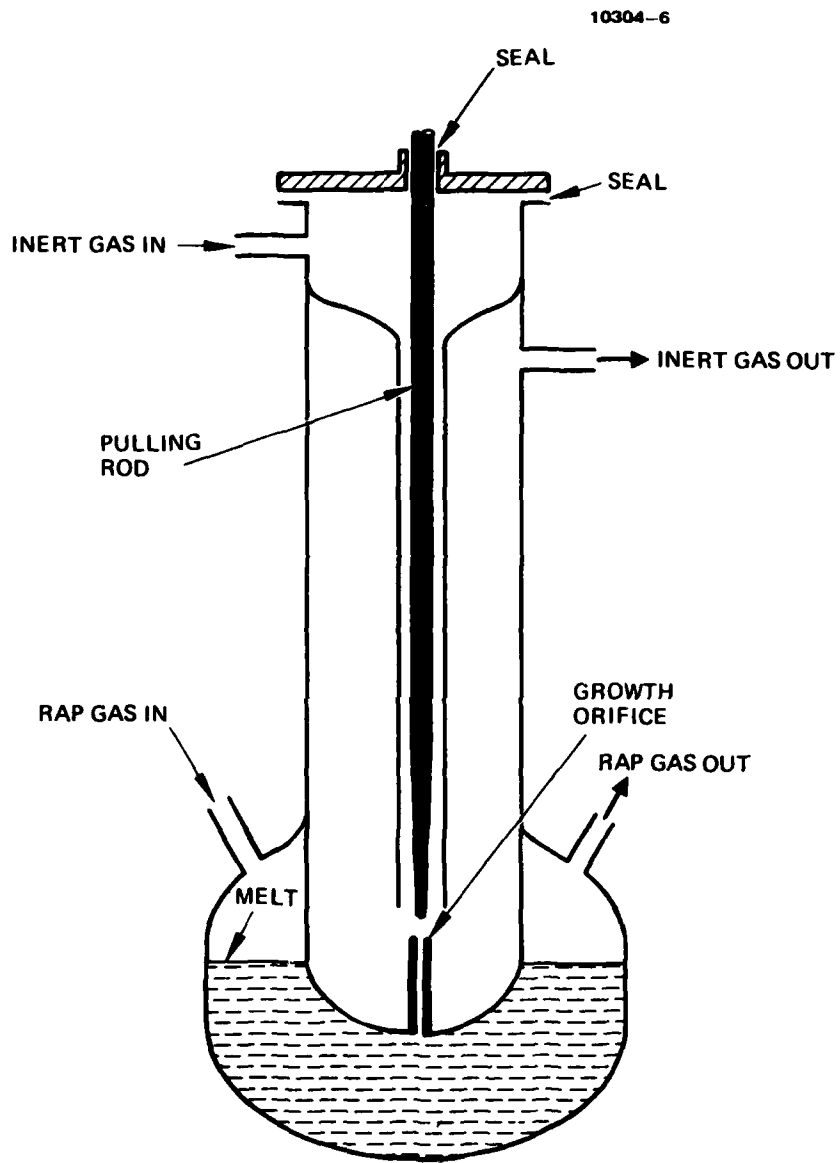ORIFICE

RAP GAS IN

RAP GAS OUT

MELT

Figure 13.   RAP-modified SC fiber system similar to
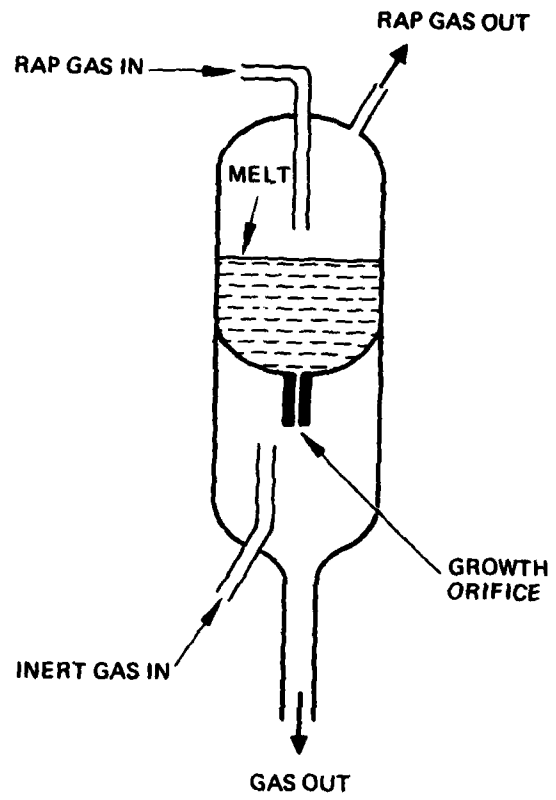   Bridges et al.[12]

10304-7

Figure 14.
Inverted Czochralski growth crucible.

41

the orifice can be controlled by adjusting the RAP gas pressure over the melt and the hydrostatic head of the melt itself. We assume that, since the exit end of the lower gas chamber is wide open, the pressure in that chamber is essentially constant at near ambient levels. The former may be regulated with a throttle valve at the exit end of the RAP gas chamber, while the latter may be determined by the amount of charge material in the melting chamber.

Several advantages of this system over the RAP-modified Bridges system are immediately evident. (1) No fiber pulling mechanism is needed, at least not for the 1-ft-long experimental specimens. (2) There is no physical limit to the length of fiber specimens that can be drawn. (3) There will be less tendency for potassium chloride vapor to condense on the glass envelope around the growth orifice.

The big question on the inverted Czochralski system is whether it is indeed possible to maintain steady-state fiber growth inside the capillary tube, that is, without the fiber pulling out due to its own weight before it becomes long enough. Unlike the situation in the Bridges system, the growth interface in the inverted Czochralski system must be within the capillary tube. How far inside it should be can only be determined by experimentation. In this respect, the Bridges system has an advantage over the inverted Czochralski system since we know that Bridges et al. were able to maintain steady-state fiber growth with it.

3. Kinetics of SC Fiber Growth

Figure 15(a) schematically represents the RAP-modified Bridge's system. If we let r be the radius of the filamentary column of molten potassium chloride, then

$$\pi r^2 \Delta P = \pi r^2 h \rho g + 2 \pi r \gamma$$

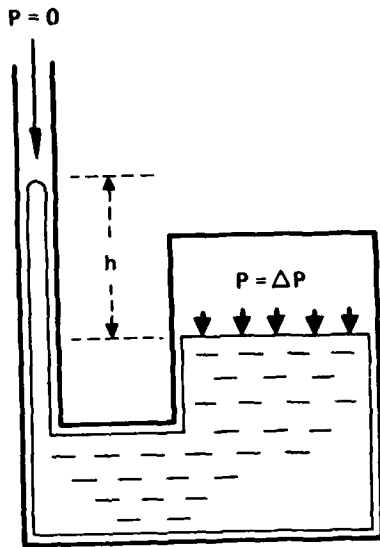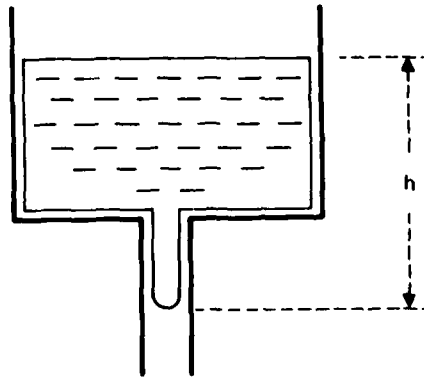$$\Delta P = h \rho g + 2 \gamma / r \quad ,$$

P = 0

h

P = ΔP

Figure 15(a).
Kinetics of RAP-modified
Bridges system for SC fiber
growth.

Figure 15(b).
Kinetics of inverted Czochralski
system for SC fiber growth.

h

43

where ρ and γ are the density and the surface tension, respectively, of molten potassium chloride at its melting point. These data (obtained from Molten Salts Handbook, Academic Press, 1967) are:

$$\gamma = 175.14 - 0.0730 \times 1043 = 99.00 \text{ dyn/cm}$$

$$\rho = 2.1359 - 0.5831 \times 10^{-6} \times 1049 - 2.1353 \text{ g/cm}^3 \quad .$$

Setting r equal to 0.015 cm yields

$$\Delta P = (2094h + 13000)\text{dyn/cm}^2 \quad ,$$

or

$$\Delta P = (1.571h + 9.751)\text{mm of Hg} \quad ,$$

where h is in centimeters. To sustain steady-state SC growth on top of the filamentary column of the melt, we estimate that fluctuations in the level of the interface $\delta \dot{R}$ should not exceed 0.01 cm. This means that pressure fluctuations δP must be held down to ~0.02 mm of mercury. Since this pressure must be maintained by a flowing gas (the RAP mixture) system, this constraint on pressure fluctuations is a severe one.*

---

* To make this more apparent, consider that effluent RAP gas must be scrubbed before it is discarded into the atmosphere. Scrubbing is achieved by bubbling the gas through a column of sodium hydroxide solution. To avoid the reverse diffusion of water vapor in the RAP outlet line, the outlet nozzle is immersed in a heavy hydrophobic liquid — a fluorocarbon compound — at the bottom of the scrubbing column. The constraint on the pressure fluctuation is equivalent to the constraint that the stream of bubbles should not be allowed to cause ripples to form on the liquid-liquid interface with amplitudes of 0.2 mm or greater.

For the inverted Czochralski system, shown schematically in Figure 15(b), the force-balance equation is:

$$\pi r^2 h \rho g = 2 \pi r \gamma \quad ,$$

$$h = 2\gamma/r\rho g \quad .$$

Using the same values of r, ρ, and γ, we obtain h = 6.3 cm. This result is to be interpreted to mean that, as long as the fluid head in the feed chamber exceeds 6.3 cm, there is no need to apply a pressure differential over the melt to cause it to flow through the capillary sink. On the other hand, the rate of flow of charge material through this capillary channel should be controllable with the temperature along that channel. For example, if the channel temperature is allowed to drop below the melting point of the charge far above the nozzle, or outlet end, the solidified charge will clog the channel and shut off flow. The ideal situation would probably be one in which there is a sharp thermal gradient on the channel so that the crystallization temperature is located just upstream from the nozzle. At this point, a balance must be established between the weight of the crystallized filament on the one hand and sur- face tension and fluid flow friction on the other if steady-state cyrstal growth is to be achieved.

4.   Results of Inverted Czochralski Growth of SC Fibers

Our attempts at the inverted Czochralski growth of KCl fibers have failed because, as hindsight now makes evident, the surface of the quartz capillary tubing was not adequately reactive atmosphere processed. This caused the surface of the tubing to remain wettable with the KCl melt, contrary to the assumption on which we had based the design of the entire inverted Czochralski fiber growing device. The contrast between the wetting and nonwetting situations at the business end of the capillary tubing is shown in Figure 16.

10304—9

WETTING   NONWETTING
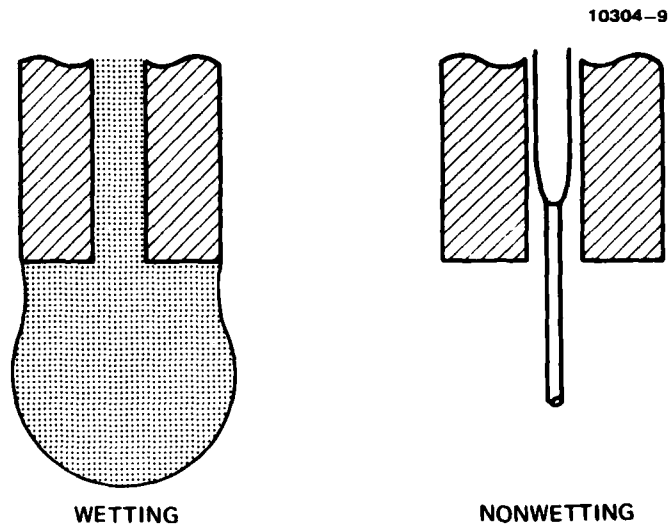
Figure 16. Sticking problems associated with
            inverted Czochralski SC fiber
            growth.

To correct for the wetting problem, we decided to RAP-coat the capillary tubing with carbon in a separate operation. Our first try at achieving this yielded a carbon coat that tended to flake off, from which we concluded that the process had been carried out too rapidly. The second RAP-coating attempt was carried out more slowly (in twice the time) and yielded a coat that was better but still with room for improvement. But unfortunately, the carbon coating was inadvertently burned off during the glassblowing operation of mounting the coated piece into the crucible. We are presently preparing for a third RAP-coating attempt.

D. FUNDAMENTAL LOSS MECHANISMS

The present losses in our best KRS-5 fibers are, as indicated in Section 2.A, far above the projected loss. Figure 1 presents projected losses for two of the most studied fiber materials, KCl and KRS-5, and for fused SiO_2 as a reference. Silica losses have now been reduced to the value of the minimum in the V curve of Figure 1. This value of 0.2 dB/km at 1.6 μm for SiO_2 has been achieved in kilometer lengths of silica fiber.[7] Therefore, to reduce loss further, we must turn to our crystalline and special glass materials.

The low energy limit (right side of V curve) to a material's transparency is multiphonon absorption. This absorption mechanism has been well studied and is known to increase exponentially as the wavelength increases toward the Reststrahl peak (one phonon cutoff). Analytically, this multiphonon edge is found to be proportional to[13]

$$\alpha_{ph} \propto \exp\left(\frac{-B\omega}{\omega_o}\right) , \tag{3}$$

where ω is the frequency of interest, ω_o is an average single phonon frequency, and B is a constant which depends on the material. In Figure 1, we plotted α_{ph} for KCl and KRS-5 using IR spectroscopic data and then extrapolated α_{ph} to obtain the curve below 10^{-3} cm^{-1}. This is the customary approach, based on Eq. 3, even though no one has verified experimentally that the multiphonon losses actually do decrease

47

exponentially beyond $\omega = 5\omega_o$. We believe, however, that this exponential behavior is a good approximation for predicting ultimate losses in the long wavelength limit.

The high energy limit (left side of V curve) on transparency is scattering loss. This loss characteristically varies as λ^{-4} for Rayleigh, Brillouin, and Raman scattering. For ideal (perfect) crystalline materials, we would expect only the contribution from inelastic scattering (Brillouin) to be significant. The attenuation coefficient for Brillouin scattering α_{sc} is given by[14]

$$\alpha_{sc} = \frac{8\pi^3}{3} \cdot \frac{kT}{\lambda^4} \cdot \frac{n^8 P_{12}^2}{\rho V^2} \quad , \tag{4}$$

where λ is the optical wavelength in free space, k is Boltzmann's constant, T is the absolute temperature, n is the refractive index, P_{12} is the Pockel's coefficient, ρ is the density, and V is the longitudinal mode acoustic velocity. Eq. 4 has been used to calculate the entire (i.e., no experimental data are used) scattering loss curve in Figure 1 for KCl and KRS-5.

The importance of the V curves for IR transparent materials is, of course, their tantalizingly low minima, which generally fall between 4 and 6 μm. We note that KRS-5 has a slightly greater minimum than KCl although it is still well below that of silica. The reason for this is the greater amount of scattering in KRS-5 due to the higher value of n (2.37 versus 1.45 for KCl at 10 μm) for KRS-5 (α_{sc}, from Eq. 4, goes as n^8). To achieve these small residual losses in fibers, we will have to eliminate all other extrinsic losses. Based on our results to date, we feel that SC fibers offer the best hope of reaching this goal because they should have the least amount of extrinsic (mechanical, chemical, and surface) absorption. Specifically, we favor the Tl halides such as KRS-5 because these materials do not cleave (cleavage steps could lead to fiber surface irregularities) and they are readily formed into fiber.

48

E. PULSE DISPERSION

An important consideration in future communication links made from these materials is pulse dispersion. The pulse dispersion arises from several sources. One source is the linewidth of the source itself and the dispersion of the material from which the waveguide is fabricated. The other source results from the guided modes (modal dispersion). We consider here the pulse spreading that arises from the dispersive nature of the material and, in particular, determine at what wavelength λ_c the guide should be operated so that the material dispersion is zero. This is the zero material dispersion (or crossover) point, and it occurs very near the minimum in the V curve for our materials.

The pulse delay τ due to dispersion in the material is proportional to the group velocity of the pulse and, therefore, to the dispersion, $dn/d\lambda$. From this it follows that the spreading of the pulse, $\delta\tau$, is related to the derivative of the dispersion, or

$$\delta\tau = \left(\frac{L\lambda}{c}\right) \frac{d^2n}{d\lambda^2} d\lambda \quad , \tag{5}$$

where L is the length of the fiber, λ is the wavelength of the light, and c is the speed of light.[15] The dispersions of most common IR materials have been tabulated. Figure 17 shows a compilation of these data taken from the AIP Handbook.[16] From these data, we can determine the value of λ when $dn/d\lambda = 0$. This is the crossover wavelength λ_c; we find that λ_c is 6.5 μm for KRS-5 and is 3.0 μm for KCl. In passing, we note that λ_c is slightly less than the minimum wavelength, λ_{min}, in the V curve for both KRS-5 and KCl (from Figure 1, λ_{min} is 6.8 μm for KRS-5 and 4.6 μm for KCl). This is also true for silica.

Using the data in Figure 17 for KRS-5, we have graphically calculated materials dispersion (for pulse spreading we need $d^2n/d\lambda^2$). These data are plotted in Figure 18. This plot of $(\lambda/c)(d^2n/d\lambda^2)$ versus λ (see Eq. 5) clearly shows the zero value for material pulse spreading which in the case of KRS-5 occurs at about 6.5 μm. Therefore, for single-mode waveguides of KRS-5 operated near 6.5 μm, there should be neither any
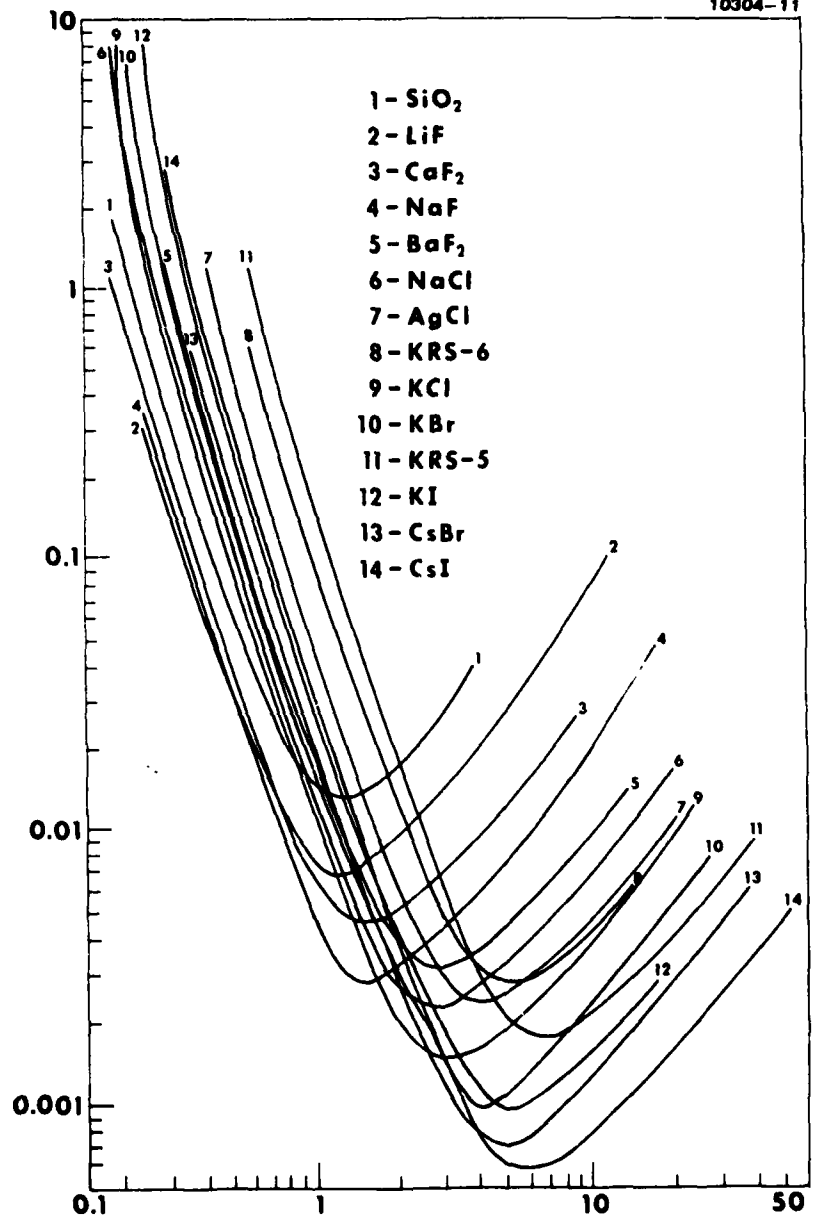
49

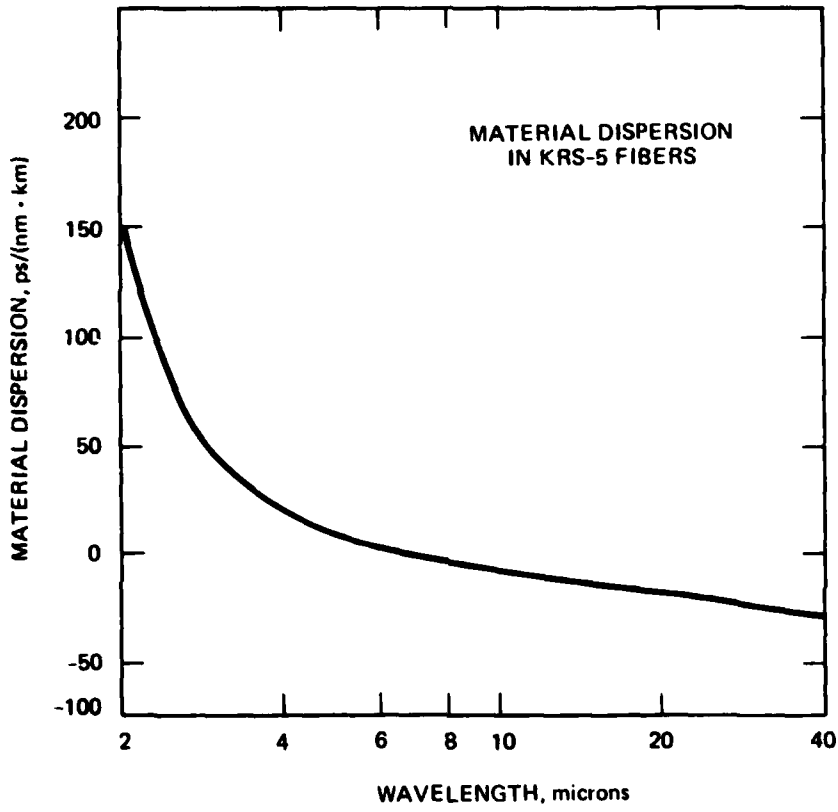Figure 17.   Dispersion versus wavelength for several
optical materials.

50

Figure 18. Material dispersion in KRS-5.

pulse dispersion due to guided modes (single mode fiber) nor any due to the material. In this ideal case, the pulse width would only be a function of the source.

F. CONCLUSIONS AND RECOMMENDATIONS

The primary purpose of this research program has been to assess the technology involved in fabricating future ultra-low-loss communication waveguides from crystalline materials. At the outset, we felt strongly that the alkali halides, especially KCl, held the greatest near-term promise for fabrication into high-quality fibers. This optimism stemmed from the availability of high-quality, bulk, single-crystal KCl, which we possessed as a result of our extensive research program in IR laser windows. Our initial approach to fabricating fiber using our RAP KCl was by extrusion. After many attempts, we were forced to abandon the extrusion process for KCl because of the poor surface quality of the fiber.

Based on these results, we decided early in the program to explore new fiber fabrication techniques for KCl. Two methods appear promising: hot-rolling and SC growth. We selected SC growth for study because SC fibers represent the ultimate low-loss fiber if they can be made. This is mainly because scattering and absorptive losses would be minimal in such an ideal waveguide. Our attempts at growing an SC fiber, however, have not as yet been successful because of technical difficulties with the apparatus. We expect our first successful results shortly.

Our theoretical calculations of projected losses in crystalline materials continue to encourage optimism for future waveguides made from materials like KCl and KRS-5. At this point, however, we recommend that work on polycrystalline fibers be terminated for this application. Instead, we feel strongly that SC fiber work should be emphasized and that most of the effort should be placed on the Tl halides. These materials are readily formed into polycrystalline fibers and do not cleave. (Cleavage cracks can occur in alkali halide fibers.) For these reasons, we believe that the next phase of this technology assessment should concentrate on SC Tl halide fibers.

REFERENCES

1. S.D. Allen and J.A. Harrington, "Optical Absorption in KCl and NaCl at Infrared Laser Wavelengths," Appl. Opt., Vol. 17, pp. 1679-1680, 1978.

2. D.A. Pinnow, A.L. Gentile, A.G. Standlee, A.J. Timper, and L.M. Hobrock, "Polycrystalline Fiber Optical Waveguides for Infrared Transmission," Appl. Phys. Lett., Vol. 33, pp. 28-29, 1978.

3. A.L. Gentile, M. Braunstein, D.A. Pinnow, J.A. Harrington, D.M. Henderson, L.M. Hobrock, J. Myer, R.C. Pastor, and R.R. Turk, "Infrared Fiber Optical Materials," in Fiber Optics: Advances in Research and Development, ed. by B. Bendow and S.S. Mitra, pp. 105-118, Plenum Publishing, N.Y., 1977.

4. J.A. Harrington, "Infrared Fiber Optics for CO_2 Laser Applications," in CO_2 Laser Devices and Applications, Proceedings of SPIE Technical Symposium East, Vol. 227, Fall, 1980.

5. R.C. Pastor and A.C. Pastor, "Crystal Growth in a Reactive Atmosphere," Mat. Res. Bull., Vol. 10, pp. 117-124, 1975.

6. L.G. Van Uitert and S.H. Wemple, "$ZnCl_2$ Glass: A Potential Ultralow-Loss Optical Fiber Material," Appl. Phys. Lett., Vol. 33, pp. 57-59, 1978.

7. S. Kobayashi, N. Shibata, S. Shibata, and T. Izawa, "Characteristics of Optical Fibers in Infrared Wavelength Region," Rev. of Elect. Comm. Lab. (Japan), Vol. 26, pp. 453-468, 1978.

8. M. Robinson, R.C. Pastor, R.R. Turk, D.P. Devor, M. Braunstein, and R. Braunstein. "Infrared-Transparent Glasses from the Fluorides of Zirconium, Thorium, and Barium," Mat. Res. Bull., to be published, 1980.

9. M. Poulain, M. Chanthanasinh, and J. Lucas, "New Fluoride Glasses," Mat. Res. Bull., Vol. 12, pp. 151-156, 1977.

10. D. Chen, R. Skogman, G.E. Bernal, and C. Butter, "Fabrication of Silver Halide Fibers by Extrusion," in Fiber Optics: Advances in Research and Development, ed. by B. Bendow and S.S. Mitra, pp. 119-122, Plenum Publishing, N.Y. 1977.

11. S. Mitachi and T. Manabe, "Fluoride Glass Fiber for Infrared Transmission," Jap. J. Appl. Phys., Vol. 19, pp. L313-L314, 1980.

12. T.J. Bridges, J.S. Hasiak, and A.R. Strnad, "Single-Crystal AgBr Infrared Optical Fibers," Opt. Lett., Vol. 5, pp. 85-86, 1980.

13. B. Bendow, "Multiphonon Infrared Absorption in the Highly Transparent Frequency Regime of Solids," in Sol. St. Physics, Vol. 3, ed. by F. Seitz and D. Turnbull, Academic Press, 1978.

14. T.C. Rich and D.A. Pinnow, "Total Optical Attenuation in Bulk Fused Silica," Appl. Phys. Lett., Vol. 20, pp. 264-266, 1972.

15. J.E. Midwinter, Optical Fibers for Transmission, J. Wiley and Sons, Inc., N.Y., 1979.

16. American Institute of Physics Handbook, D.E. Gray, editor, McGraw-Hill, N.Y., 1972.

APPENDIX

A Reprint from the

PROCEEDINGS

OF THE SOCIETY OF PHOTO-OPTICAL INSTRUMENTATION ENGINEERS

Volume 227

CO_2 Laser Devices and Applications

April 10-11, 1980
Washington, D.C.

Infrared fiber optics for CO_2 laser applications

James A. Harrington
Hughes Research Laboratories
3011 Malibu Canyon Road, Malibu, California 90265

Infrared fiber optics for CO$_2$ laser applications

James A. Harrington

Hughes Research Laboratories

3011 Malibu Canyon Road, Malibu, California 90265

Abstract

Advances in the technology of fabricating IR transmissive fiber waveguides have resulted in the development of fibers that offer unique solutions to near- and long-term IR systems problems. Short (~2 m) links of polycrystalline KRS-5 (thallium bromoiodide) fiber have already been successfully used to relay information to remote photodetectors. Future long-distance communications links may take advantage of the extremely low loss potential (~10^{-3} dB/km) predicted theoretically for a large class of IR fiber materials near 5 μm.

Introduction

Conventional (glass) fiber-optic waveguides have been successfully used in a variety of communications and military systems. Certain sensor and communications systems, however, require fiber waveguides that operate at wavelengths longer than 2 μm — the approximate cutoff of silica fibers. To meet present and future demands for highly transmitting IR fiber optics, we have fabricated IR fibers from alkali and thallium halides, which transmit IR wavelengths up to 25 μm. These materials used for fiber waveguides offer solutions to several IR systems problems, including (1) the dissection of images in the focal plane for enhanced detection and signal processing with focal plane arrays, (2) the relay of focal planes to remote photodetectors, (3) flexible transmission of high-power CO and CO$_2$ laser beams for heating and machining in remote or inaccessible locations, and (4) extremely low-loss guided communications links. We have developed KRS-5 (thallium bromoiodide) fibers that are suitable for the first three applications. Additional work in waveguide design and material purification will be required before fibers are usable for ultra-low-loss communications links. The potential for such links using halide fibers operating near 5 μm is very great since their losses are theoretically predicted to be near 10^{-3} dB/km, or a factor of 1000 better than the best glass (silica) fibers at 1.6 μm. The achievement of IR fibers with these losses would greatly affect numerous communications systems that require kilometer-long, repeaterless fiber links.

Optical Properties of IR Fibers

There are many highly transmissive IR materials,[1] but only a few have been fabricated into IR fiber waveguides. The ductile thallium[2,3] and silver[4] halides have been successfully extruded into IR fibers with fiber diameters ranging from 75 to 1000 μm. Other halides such as KCl[3] and CsI have also been extruded, but with much poorer optical quality than, for example, our best KRS-5 fiber (300 dB/km). In this paper, our emphasis will be on KRS-5 fiber since this fiber has proven to be the best fiber for CO$_2$ laser applications.

The transparency of IR materials is limited by extrinsic and intrinsic loss mechanisms. The ultimate limiting loss mechanisms in solids are multiphonon absorption[1] at long wavelengths and scattering and electronic absorptions at the shorter wavelengths. Since, at the IR wavelengths of interest (2 to 10 μm), the electronic band edge (Urbach tail) is generally a very small contributor to total attenuation,[3] the scattering and multiphonon contributions combine to give the net intrinsic loss. These losses are shown in Figure 1 for fused silica,[5] KCl,[3] and KRS-5. Each material shows a characteristic V-shape curve composed of a λ^{-4}-type scattering loss (Rayleigh/Brillouin scattering) and an exponential multiphonon tail.[1] The minimum attenuation in silica is near 1.4 μm (~0.3 dB/km), and these losses have in fact been achieved in both bulk materials and fibers[6] (i.e., the V-curve for silica has been experimentally verified). The intrinsic losses for KCl and KRS-5 are seen from Figure 1 to be considerably less than for fused silica. For these crystalline materials, as well as for other alkali halides,[3,7] TlBr,[2,3] and ZnCl$_2$ glass,[7] the minima in the V-curve is generally 1000 times less than for silica. Unlike silica, however, the measured losses in both bulk crystalline materials and fibers in these hosts is well above the intrinsic limits embodied in these V-curves. For example, the lowest-loss bulk IR material measured to date is KCl[8] (absorption coefficient $\beta = 10^{-6}$ cm^{-1} = 0.4 dB/km at 5 μm), which is still three orders of magnitude above the intrinsic limit.

IR transmissive materials have not realized this potential for ultralow loss because extrinsic absorption mechanisms (e.g., impurity, mechanical defect, and surface absorption) dominate the total attenuation. These mechanisms are important in bulk IR materials.[9] In our polycrystalline fibers, additional mechanisms (e.g., scattering from grain boundaries and irregularities in the surface of the fiber) are expected to strongly increase fiber losses. Therefore, a major task is the elimination of extrinsic sources of absorption, by, for example, using purer materials and better fiber fabrication techniques.

We have extruded polycrystalline KCl, TlBr, KRS-5, and CsI fiber using a specially built extrusion press. Extrusion temperatures were in the range of 200 to 350°C for the thallium halides and 25 to 740°C for the alkali halides. Table 1 gives the measured absorption coefficients for the extruded fibers at 10.6 μm and, for comparison, the values of the calorimetrically[8,9,10] measured loss in the bulk material (note that fiber losses are given in dB/m since this unit more accurately represents the lengths of fiber actually measured
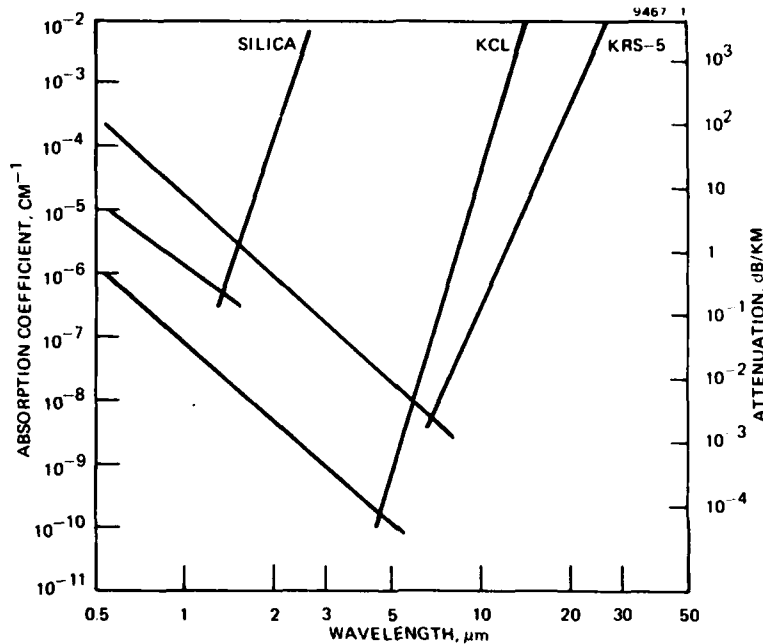
56

Figure 1. Intrinsic absorption limits in transparent materials. Short wavelength absorption is due to scattering while the long wavelength absorption is due to multiphonon process.

from 0.5 to 1.5 m). With its internal loss of ~7% per meter, KRS-5 is the best fiber material of the group. Another representation of this loss is given in Figure 2 for a 250-μm-diameter KRS-5 fiber. This fiber has an internal loss of 0.57 dB/m (external Fresnel loss for KRS-5 is 1.45 dB); extrapolating the data back to the ordinate[10] indicates that there is very little surface absorption. Extruded 500-μm-diameter KCl fiber has much higher losses because its very poor surface quality (fish-scale appearance) results in much of the light being scattered at the surface. Attempts to extrude KCl with a lubricant to reduce friction between the extrusion die and the fiber have not greatly improved the optical quality of the fiber. Results similar to those for KCl have also been obtained for CsI.

Table 1. Bulk Material and Fiber Losses at CO_2 Laser Wavelengths

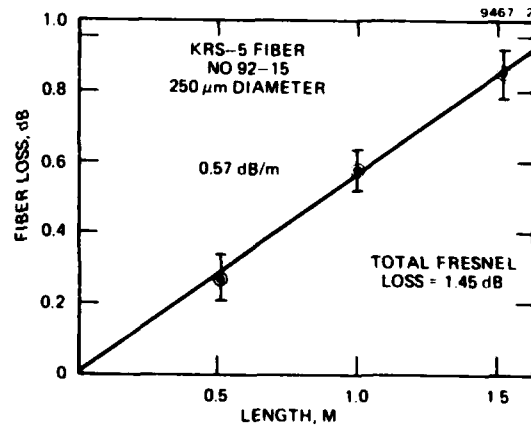| Material	Absorption Coefficient at 10.6 μm, cm^{-1} (dB/m)	
	Bulk	Fiber
KRS-5	7×10^{-4} (0.3)	7×10^{-4} (0.3)
TlBr	1×10^{-3} (0.43)	1×10^{-3} (0.43)
KCl	8×10^{-5} (0.035)	1×10^{-2} (4.2)
KBr	1×10^{-5} (0.0004)	

Figure 2. Bulk and surface absorption in KRS-5 fiber.

Measurement of the scattering losses in our fibers has been mostly qualitative. By placing liquid-crystal paper on top of a KRS-5 fiber as a means of visually inspecting the heating of a fiber irradiated with a CO_2 laser, we have found that the amount of heating observed is uniformly small over the entire length of the fiber in our best fibers. Older fibers of poorer optical quality have shown hot spots on the liquid-crystal paper or were uniformly very lossy. The hot spots can be removed — and the transmission improved — by cutting the fiber. Losses are also "visible" at points of sharp bends (<1-in. radius). When the fiber is straightened, the losses generally decrease unless the fiber has been permanently damaged (see the next section). More

quantitative experiments are underway to evaluate the scattering contribution independently by measuring the Rayleigh/Brillouin scattering spectrum of the single and polycrystalline fiber materials.[11]

The power-handling capability of KRS-5 fibers has been investigated using a CO$_2$ laser source. Figure 3 shows a 500-μm-diameter KRS-5 fiber delivering 2 W of CO$_2$ laser radiation.
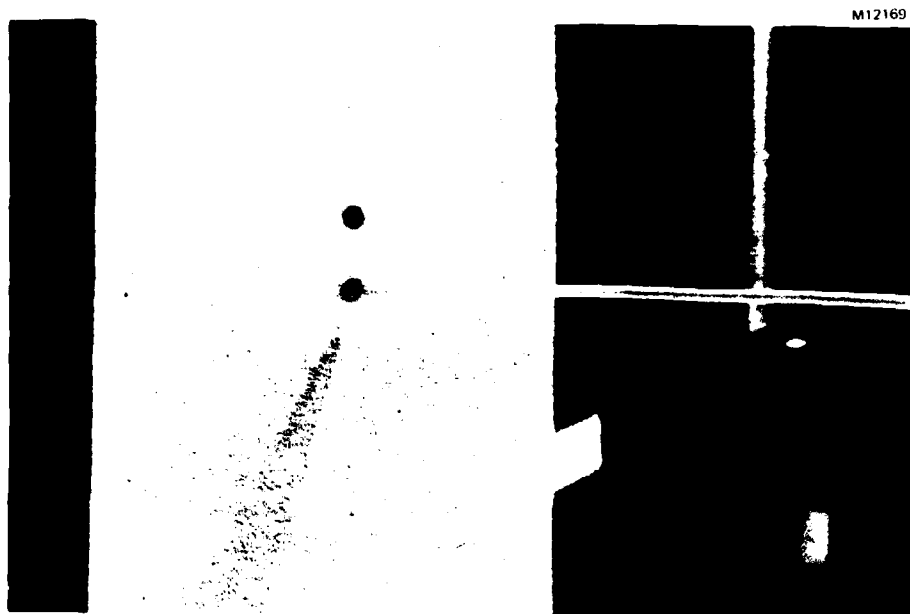

Figure 3. CO$_2$ laser power delivery by a 500-μm-diameter KRS-5 fiber.

The KRS-5 and TlBr fibers that we have been using for CO$_2$ laser applications are generally unclad. We have been unable to successfully clad the fiber using the conventional method for cladding silica fibers. Coextrusion, for example, of TlCl (n = 2.19) cladding on a KRS-5 (n = 2.37) core has produced a diffuse clad-core interface, caused by diffusion of TlCl into the KRS-5 core (along grain boundaries). This fiber had excessive losses. Similar results were obtained when post-cladding methods (such as ion exchange) were tried. The best cladding we have found has been loose-fitting polyethylene tubing. This technique works well because there is minimal contact between the fiber and the tubing[3] and thus leakage is small.

Mechanical properties of IR fibers

The extruded fibers are polycrystalline with fiber grain sizes that range between 3 and 40 μm. The grain size is a function of the extrusion temperature: the higher the temperature, the larger the grain size. Figure 4 shows 100-μm-diameter KRS-5 fiber extruded at two different temperatures.

Fiber strength is a function of fiber grain size. Yield and ultimate strength are greatest for small grain size fiber, decreasing as grain size increases (see Figure 5). Good 10.6-μm transmission has been measured for both small and large grain fibers. But the stronger, small-grain-size fiber is more desirable for most CO$_2$ laser applications. Table 2 summarizes the mechanical properties of our 100-μm-diameter fiber.

The flexural properties of IR and glass (silica) fibers are, of course, quite different. TlBr fiber is very flexible at room temperature, as shown qualitatively in Figure 6. KRS-5 fiber (250-μm diameter) may be bent to a radius of 6 in. without degradation. Warming the fiber slightly above room temperature makes this fiber even more flexible.

Fiber failure occurs when grain boundaries separate. This may be seen in Figure 7 for KRS-5 fiber. The fiber in Figure 7(a) has been stretched, revealing the separated grain boundaries (note, fiber does not neck-down). A complete break (Figure 7(b)) occurs at grain boundaries, leaving a jagged fiber end.

Applications of IR fibers

The applications of IR fibers are most easily discussed in terms of laser power transmission or the communication of information. Power applications using CO$_2$ lasers rely on the delivery of relatively small amounts of power to remote or inaccessible locations. One such use would be in laser surgery, where a flexible fiber would deliver laser radiation for applications in dentistry, neurosurgery, ophthalmology, and urology. Another power application involves laser cutting and drilling. In this use, a fiber bundle could accept CO$_2$ laser
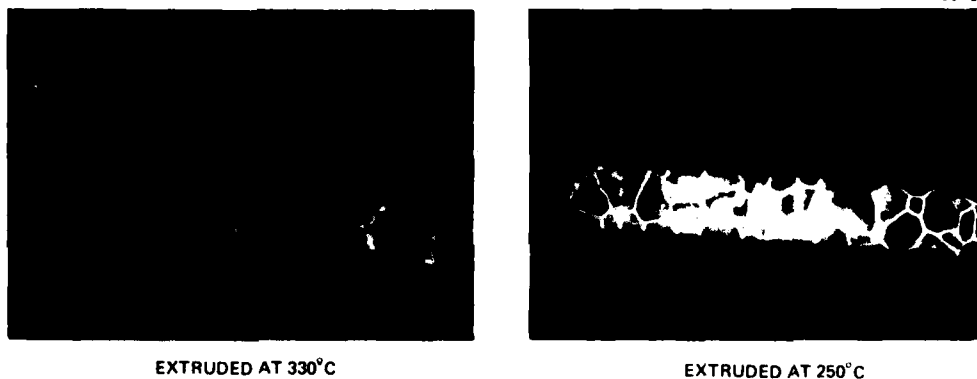
7595-23

EXTRUDED AT 330°C   EXTRUDED AT 250°C

Figure 4. Fiber grain structure in 100-μm-diameter KRS-5 fiber.

Table 2. Mechanical Properties of IR Fibers

Tensile Tests[a]	KRS-5	TlBr
Ultimate strength, psi	9000 (6)[b]	3800 (4)
Yield strength, psi	5400 (9)	3200 (4)
Elongation, %	3.1 (5)	1.2 (4)
Modulus of elasticity	1.8×10^6 (4)	0.8×10^6 (4)

[a] Tests made at 10 cm gauge length, 0.02 cm/min strain rate.

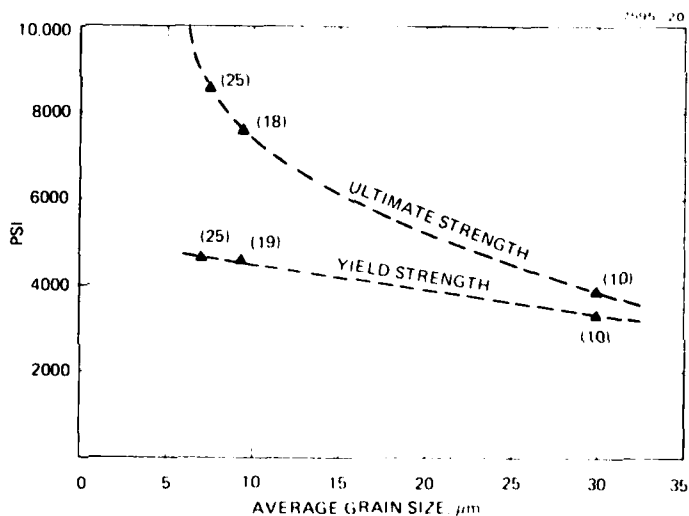[b] Number of samples tested.

Figure 5. Strength of 100-μm-diameter KRS-5 fiber as a function of fiber grain size.
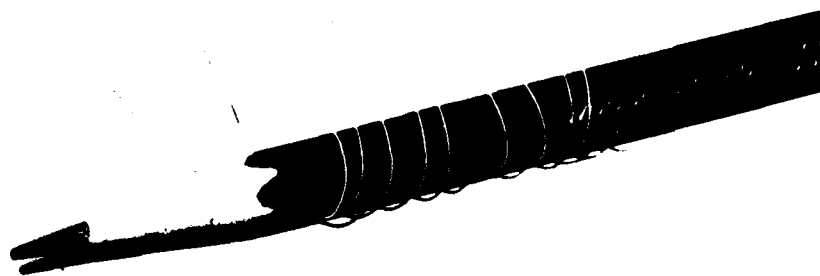
M12366

Figure 6. Coiled TlBr fiber to show flexural properties.

radiation and distribute power to remote locations. Potential uses include cloth cutting and multiple hole drilling.

The ultralow loss potential of IR fibers (see Figure 1) has enormous importance to future communications links. Fabrication of IR fiber with losses as low as 10^{-3} dB/km will allow long-distance communications systems to be built in which repeaters would not be needed. For example, an undersea (repeaterless) communication link thousands of kilometers long is anticipated. Our work on KCl fiber is directed toward understanding limiting losses in fibers and preparing ultra-low-loss IR fiber.

7721-2   7721-3

(a)   (b)
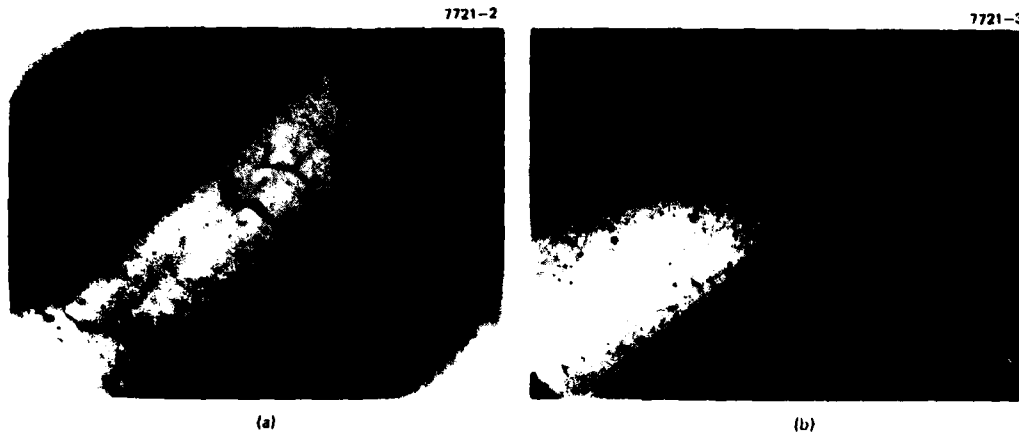
Figure 7. Mechanical failure of KRS-5 fiber.

Nearer-term applications necessarily involve shorter lengths of IR fiber (1 to 2 m). Defense systems may take advantage of the IR transparency of KRS-5 fiber (2 to 25 µm) to relay information from remote areas to photodetectors. In this application, the IR fiber would serve as a passive detector of IR radiation with the usual fiber advantages of immunity to electromagnetic interference (EMI) and resistance to jamming. We successfully tested this application by building an IR fiber receiver using two 250-µm-diameter KRS-5 fibers (each 60 cm long) to link the received signal (CO_2 laser pulses) to two cooled photodetectors. A similar application could be made in pyrometry. The long-wavelength blackbody radiation transmitted by KRS-5 fiber (near 10 µm) makes the measurement of low temperatures (less than 100°C) possible.

Conclusions

The art of fabricating IR transmissive waveguides has progressed to the point that many short-length (<10 m) applications are now possible. These applications include CO_2 laser power transmission and transmission of information at IR wavelengths. The effect on future communications systems will be great if the ultra-low-loss potential of these IR fiber materials can be realized.

Acknowledgments

The author wishes to thank D.H. Henderson, M. Braunstein, R.R. Turk, and D.A. Pinnow for helpful discussions and A. Standlee for fiber extrusion and optical measurements. This research has been supported in part by Hughes Aircraft Company IR&D programs.

References

1. Bendow, B., "Multiphonon Infrared Absorption in the Highly Transparent Frequency Regime of Solids," in Solid State Physics, ed. by Seitz and Turnbull, Academic Press, N.Y. Vol. 33, pp. 249-316, 1978.

2. Pinnow, D.A., Gentile, A.L., Standlee, A.G., Timper, A.J., and Hobrock, L.M., "Polycrystalline Fiber Optical Waveguides for Infrared Transmission," Appl. Phys. Lett., Vol. 33, pp. 28-29, 1978.

3. Gentile, A.L., Braunstein, M., Pinnow, D.A., Harrington, J.A., Henderson, D.M., Hobrock, L.M., Myer, J., Pastor, R.C., and Turk, R.R., "Infrared Fiber Optical Materials," in Fiber Optics: Advances in Research and Development, ed. by B. Bendow and S.S. Mitra, Plenum Publishing, N.Y., 1979. pp. 105-118.

4. Chen, D., Skogman, R., Bernal G, E., and Butter, C., "Fabrication of Silver Halide Fibers by Extrusion," Ibid, pp. 119-122.

5. Pinnow, D.A., Rich, T.C., Ostermayer, Jr., F.W., DiDomenico, Jr., M., "Fundamental Optical Attenuation Limits in the Liquid and Glassy State with Application to Fiber Optical Waveguides," Appl. Phys. Lett., Vol. 22, pp. 527-529, 1973.

6. Kobayashi, S., Shibata, N., Shibata, S., and Izawa, T., "Characteristics of Optical Fibers in Infrared Wavelength Region," Rev. of Elect. Comm. Lab. (Japan), Vol. 26, pp. 453-468, 1978.

7. Van Uitert, L.G. and Wemple, S.H., "$ZnCl_2$ glass: A Potential Ultralow-loss Optical Fiber Material," Appl. Phys. Lett., Vol. 33, pp. 57-59, 1978.

8. Allen, S.D. and Harrington, J.A., "Optical Absorption in KCl and NaCl at Infrared Laser Wavelengths," Appl. Opt., Vol. 17, pp. 1679-1680, 1978.

9. Hass, M. and Bendow, B., "Residual Absorption in Infrared Materials," Appl. Opt., Vol. 16, pp. 2882-2890, 1977.

10. Rowe, J.M. and Harrington, J.A., "Temperature Dependence of Surface and Bulk Absorption in NaCl and KCl at 10.6 µm," Phys. Rev. B, Vol. 14, pp. 5442-5450, 1976.

11. Rich, T.C. and Pinnow, D.A., "Total Optical Attenuation in Bulk Fused Silica," Appl. Phys. Lett., Vol. 20, pp. 264-266, 1972.

60

LIST OF ADDRESSES FOR FINAL REPORT

Maj. Harry Winsor (2 copies)
Defense Advanced Research Projects
Agency
1400 Wilson Blvd.
Arlington, VA 22209

Dr. T.G. Giallorenzi
Code 5500
Naval Research Laboratory
Washington, D.C. 20375

Dr. G.H. Siegel, Jr. (2 copies)
Code 5584
Naval Research Laboratory
Washington, D.C. 20375

Dr. R. Pohanka
Code 471
Office of Naval Research
800 North Quincy Street
Arlington, VA 22217

Naval Research Laboratory (6 copies)
Code 2627
Washington, D.C. 20375

Dr. B. Bendow
RADC/ETSS
Hanscom AFB, MA 01731

Mr. Sam DiVita
DRDCO-COM
USA CORADCOM
Ft. Monmouth, N.J. 07703

Dr. D. Albares
Code 2500
Naval Ocean Systems Center
San Diego, CA 92152

K.C. Trumble
AFAL/AAD-3
Wright Patterson, AFB OH 45433

Dr. H.B. Rosenstock
Code 5504.5
Naval Research Laboratory
Washington, D.C. 20375

Defense Documentation Center
(12 copies)

Attachment to DD Form 1423
RFP N00173-79-R-PS32

61